POLITECNICO
MILANO 1863

SCUOLA DI INGEGNERIA INDUSTRIALE
E DELL'INFORMAZIONE

Direct solar photocatalysis as an alternative hydrogen production method - current status and feasibility

Tesi di Laurea Magistrale in
Energy Engineering - Ingegneria Energetica

Author: **Morsal Babayan**

Student ID: 943616
Advisor: Prof. Giulio Guandalini
Co-advisors: Adj. Prof. Samuli Urpelainen
Academic Year: 2020-21

Abstract

Considering the daily increase in the energy consumption all over the world as well as the global warming, utilizing renewable energies is of importance. Generally renewable energy sources have a fluctuating nature which highlights the necessity of the energy storage units. Therefore, it will be possible to meet the demand by renewable energy even in the absence of the renewable source. Hydrogen is one of the clean fuels that can be produced via different fossil fuel based or renewable based mechanisms. In this study, a review of current hydrogen production methods is provided with focus on photocatalytic method which directly uses solar energy to dissociate the water molecules. Moreover, a model for solar water splitting unit consisting of a 1 [MWp] capacity monocrystalline silicon photovoltaic, a proton exchange membrane electrolysis, and hydrogen storage tanks is developed for Oulu, Finland, and Milan, Italy. Two scenarios are considered; one where the modeled system only can sell electricity to the grid ($S1$), and the other one in which the system can also purchase electricity from the grid ($S2$). It is found that the levelised cost of hydrogen for $S1$ is lower in Milan, but for $S2$ it is lower in Oulu for the electrolyser with capacity larger than 200 [kWel]. In addition, the solar-to-hydrogen (STH) conversion efficiency of the proposed system is better in Oulu for the electrolyser with capacity lower than 400 [kWel].

Keywords: Hydrogen production, Photocatalysis, Solar energy conversion, Water electrolysis

Abstract in lingua italiana

Se consideriamo l'aumento quotidiano del consumo di energia in tutto il mondo e quindi il riscaldamento globale, diventa evidente l'importanza dell'utilizzo delle energie rinnovabili. Le fonti di energia rinnovabile sono generalmente di natura intermittente, originando la necessità del loro immagazzinamento. Quest'ultimo redenderebbe possibile una corrispondenza tra la domanda e l'offerta di energia rinnovabile, persino quando la fonte dell'energia rinnovabile in questione è assente. L'idrogeno rappresenta uno dei combustibili puliti e può essere prodotto a partire da combustibili fossili o da meccanismi basati su energie rinnovabili. In questo studio presentiamo una revisione dei metodi di produzione di idrogeno più attuali, specialmente focalizzandoci sul metodo fotocatalitico, che utilizza direttamente l'energia solare per dissociare molecole d'acqua. Inoltre, è stata sviluppata ad Oulu, in Finlandia, ed a Milano un'unità per la fotolisi dell'acqua che prevede l'utilizzo di luce solare. L'unità consiste di una cella fotovoltaica basata in un monocristallo di silicio con una capacità di 1 [MWp], di una membrana elettrolitica a scambio protonico e di un sistema di immagazzinamento dell'idrogeno. Due scenari possono essere considerati. Nello scenario $S1$ l'elettricità è inviata all'unità elettrica, mentre nello scenario $S2$ può anche essere ricevuta dall'unità. Abbiamo analizzato che il costo medio dell'idrogeno in $S1$ è inferiore a Milano, ma nel caso di $S2$ è più basso ad Oulu quando si utilizza una cella elettrolitica con una capacità maggiore di 200 [kWel]. L'efficienza di conversione della radiazione in idrogeno è maggiore ad Oulu, quando si utilizza una cella elettrolitica con capacità minore di 400 [kWel].

Parole chiave: Produzione di idrogeno, Fotocatalisis, Conversione dell'energia solare, Elettrolisi dell'acqua

Contents

Introduction

The world's energy consumption has risen dramatically as a result of population growth and increased quality of living (especially in developing countries). As reported by International Energy Agency (IEA), total primary energy supply (TPES) of the world has been increased from 3.7×10^8 [TJ] to 6.1×10^8 [TJ] between 1990 to 2019. By 2050, the world population is predicted to reach a peak of 10 billion people, resulting in an even larger increase in energy demand [1]. Figure 1 presents the world's TPES by sector. The data shows that fossil fuels are yet the world's primary source of energy, despite the fact that their emissions of greenhouse gases (GHG) pollute and degrade the environment. The rise in global energy consumption has prompted further debate about clean, affordable, and long-term energy generating methods [1, 2].

Green hydrogen is one of the promising alternatives to fossil fuels. Due to hydrogen's uncomplicated electrochemical conversion, high mass energy density, and light weight, transporting energy in the form of liquid fuels is also practical [3]. Hydrogen is a well-known and efficient energy carrier that can be derived from both renewable and nonrenewable resources. Therefore, it is feasible to have no greenhouse gas (GHG) emissions if the hydrogen production procedure is carried out with renewable energy sources (RES). Moreover, besides the energy source, material source of hydrogen is of importance. Resources containing the hydrogen element, e.g. water, carbohydrates, and hydrocarbons, are converted to hydrogen and other byproducts. Even though water is the most clean source to produce hydrogen, nowadays, nearly 96% of hydrogen is derived from conventional fossil fuels, with 30%, 48% and 18% coming from naphtha reforming, natural gas steam reforming, and coal gasification, respectively [4].

Although hydrogen is the most abundant element, it is not available in the nature in its fuel form. To address this issue, a wide range of technologies are developed which can be divided into two groups of conventional and renewable methods, based on their raw materials. Conventional methods, including different hydrocarbon reforming methods, coal gasification, and pyrolysis utilize fossil fuels to produce hydrogen. On the other hand, renewable methods employ renewable resources such as water and biomass. Thermolysis, electrolysis and photo-electrolysis are renewable methods operating with water split-

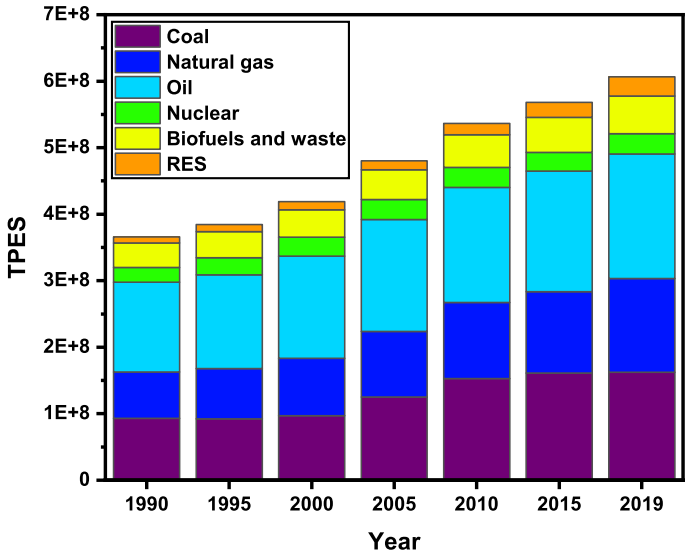

Figure 1: World total primary energy supply (TPES) [1]

ting reaction. For biomass as the feedstock, thermochemical and biological processes are developed. Biomass gasification, pyrolysis, combustion and liquefaction are main thermochemical processes, while direct and indirect biophotolysis, dark fermentation, and photo-fermentation are the biological ones [5].

Solar energy is the most abundant renewable energy freely available all over the world which can be used in various applications such as water treatment and generating electricity and thermal energy [6, 7]. In fact, one hour of sunlight produces more energy than humans consume in an entire year [8]. Furthermore, numerous solar-driven hydrogen production methods have been developed that can be categorized as photocatalytic (PC), photoelectrochemical (PEC), photovoltaic–electrochemical (PV-EC), and solar thermochemical (STC) water splitting, as well as photothermal catalytic (PTC) hydrogen production from fossil fuels (mainly CH_4) and photobiological (PB) hydrogen production [9].

According to Global Hydrogen Review 2021 published by IEA [10], fossil fuel-based hydrogen almost entirely met the global hydrogen demand of 90 [Mt] in 2020. Owing to the dominance of the fossil fuel consumption, hydrogen production is in charge of approximately 900 [Mt] direct CO_2 emissions in 2020. Sustainable hydrogen production technologies were surprisingly strong throughout the COVID-19 epidemic and it was a record year for policy action and low-carbon production. For example, in 2020, 70 [MW] of electrolysis capacity was installed (25 [MW] in Peru, 20 [MW] in Canada, and 10 [MW]

in Japan were the largest ones) which doubled the record of 2019. Additionally, two fossil fuel-based hydrogen producing units with Carbon Capture, Utilization, and Storage (CCUS) became operational with 320 [kt] of low-carbon hydrogen in Canada during 2020 [2, 10].

In this study, a brief review of major hydrogen production methods based on their source of energy is presented. Then the photocatalytic hydrogen production which is a promising method to generate hydrogen directly by solar energy is explained in details. Also several types of photocatalyst materials considered for hydrogen production has been discussed. Finally, feasibility analysis of a solar water splitting unit consisting of a photovoltaic plant, and a water electrolysis is developed for Oulu, Finland, and Milan, Italy. Then, based on the calculated levelised cost of hydrogen, the investment cost of the photocatalytic water splitting is calculated as the breakeven reference cost for this technology.

1 | Hydrogen production methods

Hydrogen production technologies are to be designed and developed so as to produce molecular hydrogen (H_2) from hydrogen containing resources where the hydrogen is chemically bound. Hydrogen production methods can be categorized depending on the type of the utilized raw material and the type of the energy source driving the conversion. In this chapter various hydrogen production methods are categorized and briefly described based on the utilized energy source. To produce hydrogen one can employ one or combination of *thermal*, *electrical*, *photonic*, or *biochemical* energy forms. Apart from green sources such as solar, wind, geothermal, etc., the required energy can be obtained from fossil fuels in which all produced carbon dioxide must be processed (separated, sequestrated, etc.) to be considered as the green hydrogen production.

1.1. Thermal Methods

Hydrogen production methods with thermal processes as the driving energy are the most common ones [11]. In this method, heat energy is converted to the chemical energy in the form of hydrogen. considering the source of the heat, the produced hydrogen might be green or not. Solar energy, nuclear energy, and fossil fuel-based units with CCUS can be utilized in thermal methods to produce green hydrogen. Thermal methods are classified in various subsection listed below.

1.1.1. Thermolysis

The direct thermal decomposition of water molecules to hydrogen and oxygen known as thermolysis is a one-step reversible reaction.

$$H_2O \xrightarrow{\text{Heat}} H_2 + \frac{1}{2} O_2 \; \Delta H_{300\ [K]} = 286\ [kJ/mol] \tag{1.1}$$

A high temperature heat source is indispensable to obtain high degree of dissociation in this method. At atmospheric pressure, dissociation levels of 4% and 64% are reported

for 2500 and 3000 [K] heat sources respectively [12, 13]. To ensure the green hydrogen production, renewable high temperature energy sources such as concentrated solar power (CSP) can be utilized. Considering the operational conditions for this method, the reactor must be made of high-temperature resistant materials which increases the cost of the equipment. Additionally, separation of produced hydrogen and oxygen is also a challenge to overcome in this method.

1.1.2. Thermochemical water splitting

Even though thermolysis could capture enough attention during the 70s and early 80s, to overcome the related high temperature issues for hydrogen production, decomposition of water with the aid of repetitive series of chemical reactions known as thermochemical water splitting were developed [14]. There is no need for catalysts in these reactions and all utilized chemicals are recycled except for water which is the source of the produced hydrogen. Compare to thermolysis in which the required temperature is in the range of 2500 to 3000 [K], thermochemical water splitting operates in feasible temperature range (600 to 1200 [K]). Zero or low electrical energy demand and no need for separation of H_2 and O_2 are other features of this method that have made it a promising way to produce green hydrogen [15]. By 2006, more than 280 thermochemical water splitting cycles were revealed for hydrogen production reported by Argonne national laboratory (ANL) [16].

The most well-investigated and popular thermochemical water splitting cycle is the sulfur-iodine (S-I) cycle that is proposed by General Atomics as a promising method to produce green hydrogen. The maximum operating temperature in this cycle is around 1120 [K] which can be supplied by nuclear heat sources, CSP, and biomass consumption [17]. The S-I cycle equations are listed below [18]:

$$H_2SO_4 \longrightarrow H_2O + SO_2 + \frac{1}{2}\,O_2 \text{ at } 1120\ [K] \tag{1.2}$$

$$I_2 + SO_2 + 2\,H_2O \longrightarrow 2\,HI + H_2SO_4 \text{ at } 400\ [K] \tag{1.3}$$

$$2\,HI \longrightarrow H_2 + I_2 \text{ at } 400\ [K] \tag{1.4}$$

Yilmaz and Selbaş [17] have done a thermodynamic energy and exergy performance assessment of a Sulfur-Iodine (S-I) thermochemical unit assisted with solar energy. They have reported 43.85% and 62.39% energy and exergy efficiency for the S-I cycle, respectively. However, the energy and exergy performance of the whole system is calculated to be 32.76% and 34.56%, in the given order. With this results they believe that S-I thermochemical cycle is a feasible technique to produce hydrogen in future.

1.1.3. Gasification

Biomass gasification

Municipal or agricultural solid carbonaceous waste (known as biomass) such as sugar cane bagasse and wood sawdust can be utilized to produce sustainable and green hydrogen with low emission of carbon dioxide [15, 19]. Biomass is oxidized within a gasifier at a high temperature and transformed into a gaseous mixture containing hydrogen, methane, carbon monoxide and carbon dioxide. This process known as biomass gasification is the most efficient and economic hydrogen production method. While the biomass to hydrogen efficiency, based on lower heating value (LHV), for this process is reported to be almost 69%, its overall energy efficiency can reach 90% with the aid of energy recovery units [20, 21]. The performance of this method depends on operational parameters, including reactor type, the feedstock, and operation temperature [22, 23]. Temperature range of 700 to 1200 [K] and air, oxygen or steam as the gasifying agent are required. Despite the higher energy cost, the product of the steam gasification has higher heating value and superior hydrogen production in comparison with air gasification. Moreover, high-cost oxygen separation process is not required in the case of the steam gasification [24, 25]. Whenever the moisture content of the biomass is too high (e.g. wastewater), it must be dehydrated prior to gasification or the supercritical water gasification (SCWG) can be employed. In this process, apart from biomass, water is also a source of hydrogen production. Water must be in its supercritical condition ($P > 22.1$ [MPa] and $T > 647.1$ [K]), therefore lower operational temperature is demanded [26].

Coal gasification

As the most abundant fossil fuel, coal could be a promising source to produce hydrogen usually through gasification. Even though the efficiency of coal gasification is lower than the steam methane reforming , it is an economical and practical option particularly where the coal is more affordable than methane. Currently 18% of the total hydrogen production in the world is produced using this method [27, 28].

The gasification occurs within the gasifier where the dried coal is oxidized in the presence of oxygen and steam at high pressure and high temperature condition. In this process syngas (a mixture of H_2, CO and CO_2) is produced. The corresponding reactions are [29]:

$$C + O_2 \longrightarrow CO_2 \; \Delta H = -405.9 \; [kJ/mol] \tag{1.5}$$

$$C + H_2O \longrightarrow H_2 + CO \; \Delta H = 118.9 \; [kJ/mol] \tag{1.6}$$

The gas mixture then enters the water gas shift reaction in which the produced CO turns into CO_2 besides enhancing the hydrogen yield. In order to increase the overall efficiency of the plant, a part of the produced syngas can be used to generate electricity with the aid of gas turbines.

Considering high CO_2 emissions, coal gasification possesses the highest global warming potential among all hydrogen production processes [30]. To address the environmental effects, CCUS technologies should be applied which leads to higher capital costs, ergo high-cost hydrogen production [13]. Therefore, development of CCUS technologies is indispensable to have a competitive hydrogen production by coal gasification [31].

1.1.4. Reforming

Fossil fuel reforming is a viable option to produce hydrogen. CO and CO_2 besides H_2 are also emitted in this method. Partial oxidation, steam reforming, and autothermal reforming are the main reforming technologies. In partial oxidation, the fuel is oxidized partially in the absence of any catalyst. Unlike the partial oxidation in which the reaction itself provides the required heat, an external heat source is demanded for steam reforming. However, no need for oxygen, and lower operating temperature besides higher H_2 to CO ratio are the advantages of steam reforming over partial oxidation and autothermal reforming. Autothermal reforming has lower operating pressure in comparison with partial oxidation. Although there is no need for external heat source for autothermal reforming, similar to partial oxidation, pure oxygen demand for reaction and consequently oxygen separation unit for products increases the cost of the produced hydrogen [13].

Among all reforming technologies, steam methane (natural gas) reforming (SMR) is the most widely used hydrogen production method with 48% share of world's hydrogen production. Methane is a more favorable fuel for steam reforming, because of its high hydrogen-to-carbon ratio which leads to less undesired by-products [4, 32]. Despite the high global warming potential of SMR, it produces low cost hydrogen (less than 2 [$/kg]) in comparison with other hydrogen production methods [33]. The SMR consists of two steps: a reforming reaction and a shift reaction.. Methane and steam are mixed during the reforming step in the presence of a catalyst at 1.5 to 3 [MPa] pressure and $900-1200$ [K] temperature. At this stage, CO and H_2 are the products. During the second step (i.e. the shift reaction), the produced CO reacts with the excess steam producing more H_2 as well as CO_2 [34]. Therefore, to produce green hydrogen, it is mandatory to capture the

emitted carbon dioxide with the aid of CCUS methods.

$$CH_4 + H_2O \longrightarrow CO + 3\,H_2 \tag{1.7}$$

$$CO + H_2O \longrightarrow H_2 + CO_2 \tag{1.8}$$

1.2. Electrical Methods

Electrical hydrogen production methods, or water electrolysis, are considered as means to convert electric power into chemical form [35]. Similar to thermolysis, pure hydrogen and oxygen are the only products of water electrolysis, however, a DC current is the energy source providing the required significant amount of the energy. Two half-cell reactions of the oxygen and hydrogen evolution reactions (i.e., OER and HER) occur at the anode and cathode almost at constant pressure and temperature respectively [2, 15].

$$\text{Anode}: H_2O \longrightarrow \frac{1}{2}\,O_2 + 2\,H^+ + 2\,e^- \tag{1.9}$$

$$\text{Cathode}: 2\,H^+ + 2\,e^- \longrightarrow H_2 \tag{1.10}$$

$$\text{Overall}: H_2O \longrightarrow H_2 + \frac{1}{2}\,O_2 \tag{1.11}$$

Even though, electrolysis is the first utilized method to synthesize hydrogen [36], it only contributes 4% to the global hydrogen production, due to its lower efficiency and higher cost in comparison with SMR and CG [31]. Movement of the electrons driven by an external circuit is the base of this method. Therefore the current density besides the efficiency is of importance for water electrolysis. Here, the efficiency is defined based on the ideal and real energies required to drive the reaction. To enhance the current density and the reaction rate, catalysts (normally Platinum) are often used. [13, 15]

Based on the utilized electrolyte system, electrolyzers are classified into alkaline water electrolysis (AWE), proton exchange membranes electrolysis (PEMs), solid oxide water electrolysis (SOE), and anion exchange membranes electrolysis (AEMs) [28, 37, 38]. Electrolysis can also be classified based on their operating temperature as the low-temperature electrolysis (LTE) with working temperature of $340 - 360$ [K], and the high temperature electrolysis (HTE) with working temperature of $970 - 1270$ [K] [39]. The advantage of HTE over LTE is that it makes use of both electrical and thermal sources, consuming less electricity and producing almost zero emission of GHG in the presence of external clean heat source [40].

1.2.1. Low temperature electrolysis (LTE)

AWE and PEM electrolyzers known as the LTEs, are the most commonly used electrical methods to generate hydrogen in large scale [41]. Two non-platinum metals as the electrodes, a diaphragm membrane, and an electrolyte with $30-40\%$ potassium hydroxide (KOH) are the main components of the AWE (Figure 1.1a). No need for a noble metal catalyst as well as easy handling due to lower temperature are advantages of this method. The AWE is considered as the promising method to produce hydrogen up to megawatt scale [42–44].

PEM electrolyzers are similar to the AWE expect they have a solid polymer membrane as the electrolyte in which the protons (i.e. hydrogen ions) act as the charge carriers (Figure 1.1b) [45]. PEM electrolyzer can be both employed to generate hydrogen, and be used in fuel cells which use hydrogen as the fuel to produce electricity [2]. At the anode, water splits into oxygen and protons that are transferred to the cathode through the solid electrolyte to react with electron and produce hydrogen [46]. Even though the efficiency of the PEM electrolyzer is higher than AWE, the necessity of noble metals such as platinum and iridium besides the degradation of its electrolyte have made the AWEs more widespread than PEMs [42, 43, 47]. Based on the IEA report, 61% and 31% of the installed water electrolysis capacity in 2020 belong to AWE and PEM electrolyzers respectively [10].

1.2.2. High temperature electrolysis (HTE)

In comparison with LTEs, SOE electrolysis produce hydrogen from steam or water at high temperature with higher energy efficiency and operating power [48]. Apart from the electricity, thermal energy is also needed in SOEs to drive the reaction as given in Equations (1.12) and (1.13) [31, 43]:

$$H_2O + 2\,e^- \longrightarrow H_2 + O^{2-} \tag{1.12}$$

$$O^{2-} \longrightarrow \frac{1}{2}\,O_2 + 2\,e^- \tag{1.13}$$

SOE electrolysis is in early development and is not commercially available yet. However, its low estimated cost (by 2050) and its capability to operate in the inverse process to produce electricity (solid oxide fuel cells, SOFC) have made it a promising method to produce hydrogen in large scale in the future [31].

The other HTE method, i.e. AEM, is designed in the way that contains advantages of

both alkaline and PEM electrolysis simultaneously. In this technique, an anion exchange membrane is utilized as the electrolyte besides two catalyst-based metals such as platinum and iridium as the electrodes [49]. The low capital cost of the AEM electrolysis can help the large scale hydrogen production become a reality [44]. Although, AEM electrolysis is principally similar to PEM electrolysis, hydroxyl ions carry the charge instead of protons, as presented in Figure 1.1d. The reactions happening within an AEM electrolysis are [44]:

$$2\,H_2O + 2\,e^- \longrightarrow H_2 + 2\,OH^- \tag{1.14}$$

$$2\,OH^- \longrightarrow \frac{1}{2}\,O_2 + H_2O + 2\,e^- \tag{1.15}$$

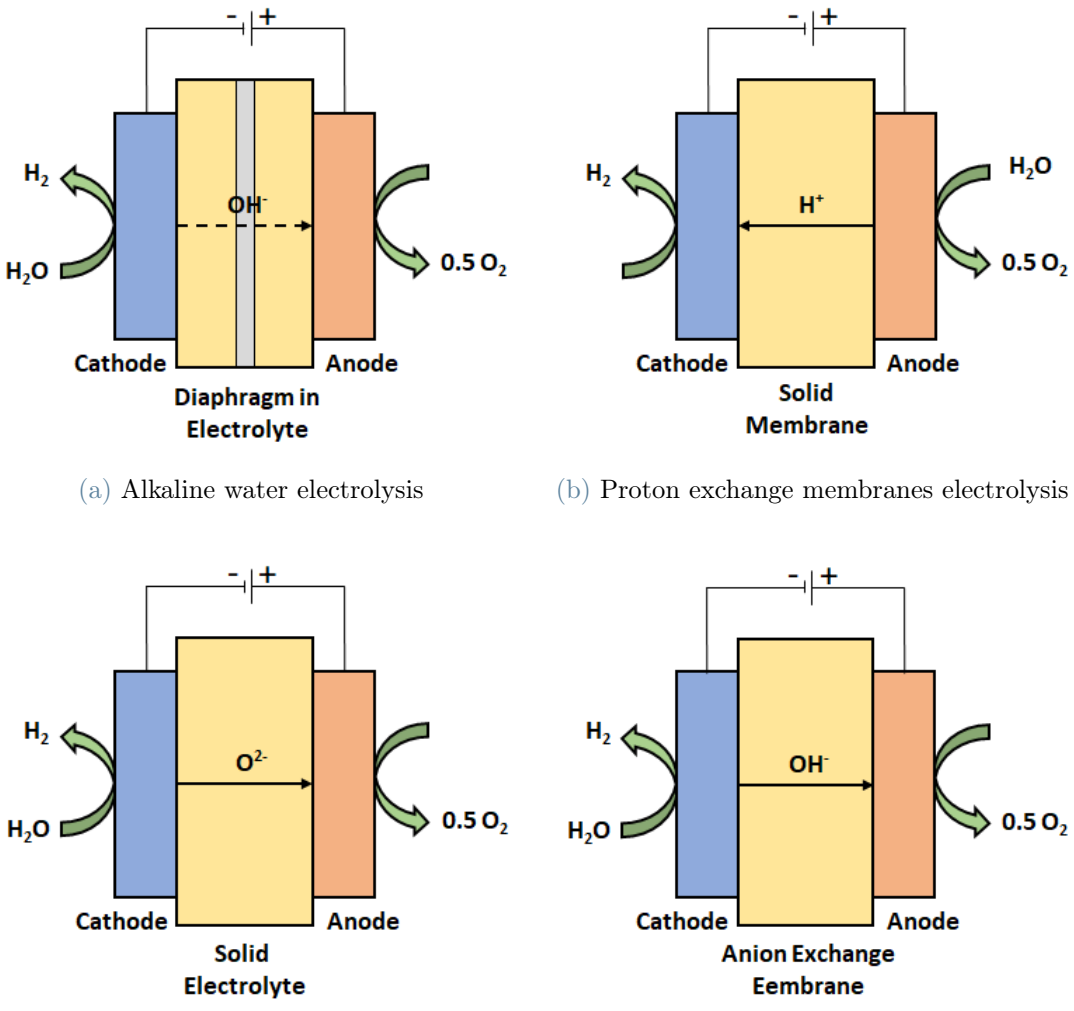

(a) Alkaline water electrolysis

(b) Proton exchange membranes electrolysis

(c) Solid oxide water electrolysis

(d) Anion exchange membranes electrolysis

Figure 1.1: Schematic diagram of various electrolysis.

Primary energy sources such as fossil fuels and renewable energies are used to generate secondary ones like electricity and heat. Fossil fuels including coal, natural gas, and oil are the primary energy source for more than 60% of the world's total electricity generation [1]. Therefore, in order to produce green hydrogen by water electrolysis, electricity generated by renewable sources such as solar photovoltaic, nuclear, and wind must be employed [31]. As reported by National Renewable Energy Laboratory (NREL), in major part of the United State, the cost of hydrogen production by electrolysis is comparable with gasoline [50].

1.3. Photocatalytic Methods

One clean source of energy that can provide the required energy for water dissociation is solar radiation. Therefore, photocatalysis is a way of converting and storing the solar energy in the form of chemical energy using suitable catalysts (i.e. semiconductor) [51]. In addition to water, organic substrates like methanol, ethanol, as well as aromatic water pollutants can also be used as the source of the hydrogen through similar processes known as photoreforming processes [52, 53]. Photocatalytic methods has also the capability to be used in water treatment technologies to remove organic pollutants from wastewater. Besides clean water as the main product, hydrogen is a valuable byproduct of photocatalytic degradation of contaminants [54, 55].

The solar radiation spectrum at the top of the earth's atmosphere as well as at sea level is depicted in Figure 1.2. The distribution of the solar light is similar to that of the blackbody with approximately the surface temperature of the sun (5520 [K] temperature) [56]. The solar spectrum can be divided into three sections of ultraviolet light (wavelengths less than 400 [nm]), visible light (wavelengths between 400 to 760 [nm]), and infrared (wavelengths larger than 760 [nm]). While 38.9% of the sunlight at top of the atmosphere is visible light, 6.8%, and 54.3% of it is comprised of ultraviolet (UV) and infrared (IR) respectively [57]. However, as light passes through the atmosphere, it loses a portion of its power due to Rayleigh scattering, dust and aerosol scattering, cloud surface reflection, and absorption by water, oxygen, and carbon dioxide. Therefore, at the sea level, solar spectrum is divided in 6% of UV light, 48% of visible light, and 46% of IR light [58].

It is known that the energy of the photon is correlated to the frequency of the radiation as below:

$$E_{photon} = h\nu \tag{1.16}$$

in which, ν, and h are the frequency of the radiation and the Plank constant respectively.

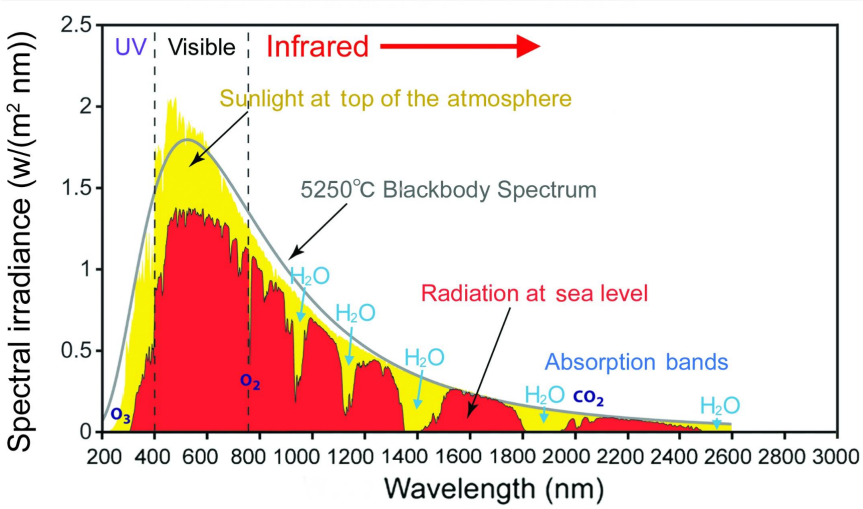

Figure 1.2: Solar Spectrum. Reproduced with permission from reference [56]

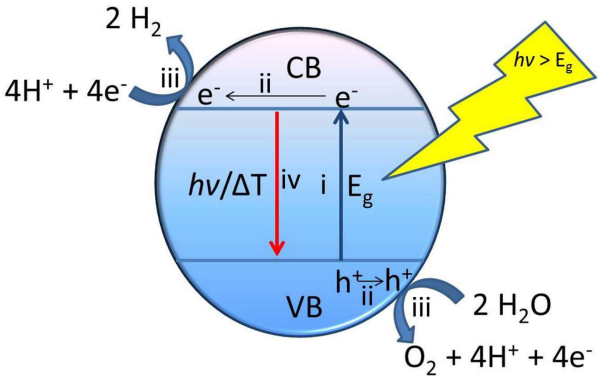

Figure 1.3: Photocatalytic water splitting stags. (i) photo-induced charge generation, (ii) charge migration, (iii) photochemical reactions and (iv) charge recombination. Reproduced with permission from reference [59].

In a photocatalytic process, solar radiation is absorbed by the photoelectrodes made of a semiconductor. Similar to a photovoltaic (PV) cell, an electron-hole pair is generated when the absorbed photon has energy higher than the band gap energy of the semiconductor. However, in photocatalytic methods, the generated electrical charge is directly used to dissociate water as opposed to electrolysis using solar energy, where the solar energy would be first converted into an electric current driving the reaction at the electrode. Therefore, there is no need for a distinct power generation like PV that makes it a more compact solution [13]. Different stages of the photocatalytic water splitting reaction are depicted in Figure 1.3.

In this type of hydrogen production method, the utilized catalyst should have the following criteria [51]:

- absorb visible light (display suitable band gaps)
- be chemically stable under redox conditions
- be chemically resistant
- have a low cost
- be recyclable
- be adaptable for large-scale hydrogen production

So far, various types of photosensitive semiconductors are studied in which, titanium oxides, cadmium sulfides and zinc oxide/sulfides are expressed as the most efficient ones for hydrogen production by means of photocatalytic water splitting [13, 14]. Due to the accessibility, and affordability of titanium dioxide (TiO_2) besides its chemical resistance properties, it has attracted more attention [60]. Studies have shown that addition of different metals, particularly earth-abundant ones such as Ni and Cu, can enhanced the hydrogen production [61–64]. Although the global worming potential is the lowest for this method, the need for sacrificial reagents which have environmental impact, low visible light activity of photocatalysts, low exergy efficiency, and the high cost are the disadvantages which make it less favorable [11, 14].

1.4. Biological Methods

Hydrogen production from biomass or solar energy with the aid of microbial species such as hydrogenase or nitrogenase enzymes are known as the biological methods which is usually done at ambient pressure and temperature. Biological methods can be classified as light dependant methods, i.e. direct or indirect biophotolysis and photo-fermentation, and light independent ones, i.e. dark-fermentation [65]. Bio-photolysis benefits from photosynthetic reaction to split water into hydrogen and oxygen in the presence of solar energy in both direct and indirect mood. Cyanobacteria and microalgae are used in this method to drive the photosynthetic reaction in specific photo-bioreactors. The direct bio-photolysis consists of one step to dissociate water into hydrogen, while during the indirect one, at the first stage water is used to produce glucose which then is transformed into hydrogen [11].

Besides photosynthetic bacteria, anaerobic ones like Rhodobium and Rhodobacter can also be employed in the presence of solar energy to generate hydrogen from organic compounds through photofermentation in which nitrogenase-catalyzed reaction is the driven reaction [66]. The absence of oxygen evolving reactions and consequently no need for oxygen

separation, high substrate conversion yields, capability of using varied range of sunlight, and possibility of combining this method with waste disposal are the main advantages of photofermentation [2].

Organic and waste materials can be utilized to produce hydrogen by using anaerobic organisms even in the absence of the solar energy known as dark-fermentation [67]. Lower estimated production cost and required energy have made dark-fermentation a promising technique to produce hydrogen. However, similar to photo-fermentation, it is sensitive to a series of process parameters including the type of the organism, reaction temperature, pressure, etc. which has been studied to optimize the hydrogen production [11, 14]. Moreover, It is shown that higher total hydrogen yield is feasible by a hybrid system with dark-fermentation as the first stage and photo-fermentation as the second one [68].

1.5. Solar-driven hydrogen production

Hydrogen production methods are introduced and developed so as to address the climate change and air pollution by replacing the fossil fuels with a clean fuel. On the other hand, solar energy is the most abundant and almost easily available renewable energy all over the world. Therefore, solar hydrogen production has the potential to tackle these issues by harvesting solar energy and store it in the form of chemical energy to be used whenever it is needed. Photocatalytic water splitting, photoelectrochemical water splitting, photovoltaic–electrochemical water splitting, solar thermochemical water splitting, photothermal catalytic hydrogen production from fossil fuels (mainly CH_4), and photobiological hydrogen production methods are the main solar-driven hydrogen production techniques.

Photocatalytic water splitting is briefly explained in Section 1.3 and will be explained more in the next chapter. Solar thermochemical water splitting and photothermal catalytic hydrogen production from fossil fuels are the thermochemical water splitting and reforming hydrogen production that solar energy provides the required thermal energy. These methods are explained in Sections 1.1.2 and 1.1.4, respectively. Photobiological hydrogen production consists of bio-photolysis and photofermentation which are mentioned in Sections 1.4.

Photoelectrochemical water splitting employs both solar and electrical energy to produce hydrogen. This is commonly done using n/p-type semiconductor-based photoanode/photocathode for oxygen/hydrogen evolution (i.e., OER and HER) reaction as well as a counter electrode for the other half-reaction. In a photoelectrochemical cell with n-type semiconductor-based photoanode (see Figure 1.4b, left), light is irradiated on pho-

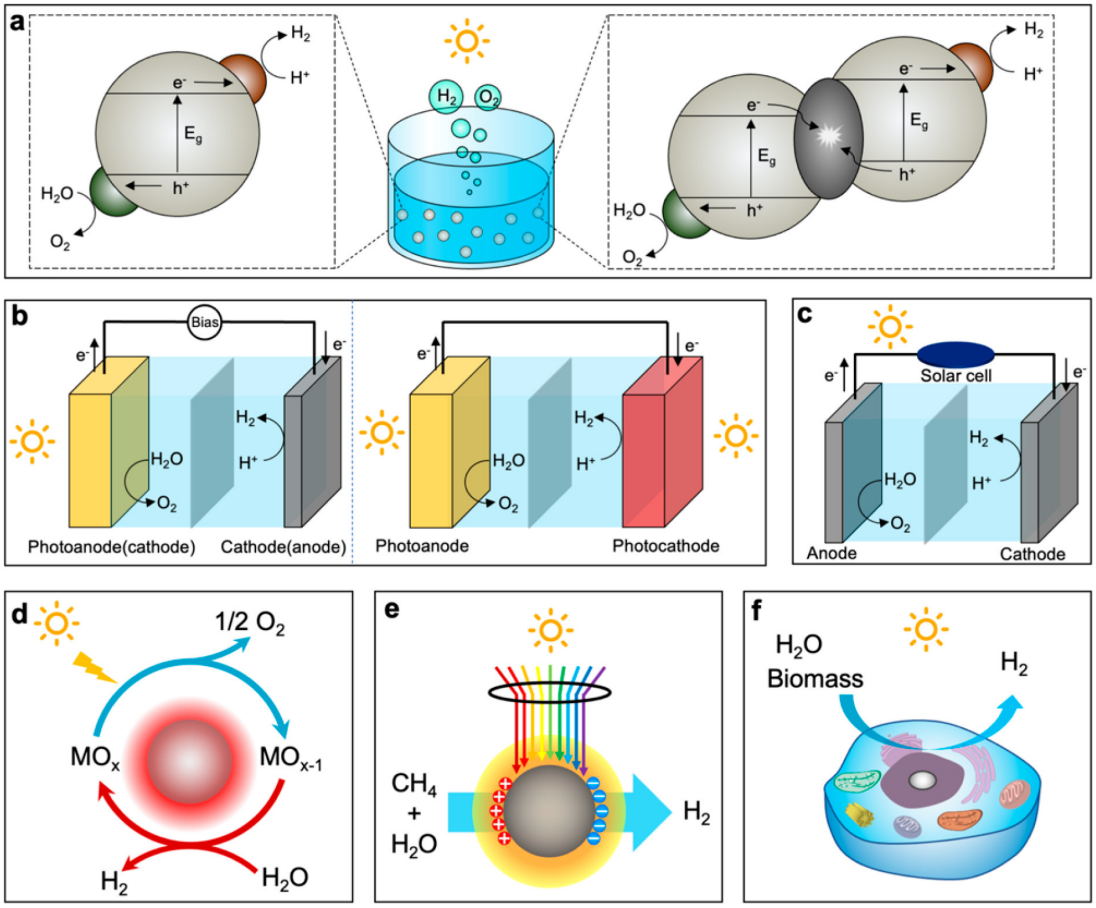

Figure 1.4: Various solar-driven hydrogen production approaches: (a) photocatalytic water splitting, (b) photoelectrochemical water splitting, (c) photovoltaic–electrochemical water splitting, (d) solar thermochemical water splitting, (e) photothermal catalytic hydrogen production, and (f) photobiological hydrogen production. Reproduced with permission from reference [9].

toanode, generating electron-hole pairs within the anode. While the holes (hydrogen ions) transfer to the surface of the anode to drive the OER, the electrons migrate through the external circuit towards the cathode to drive the HER. As presented in Figure 1.4b, right, by combining a photoanode and a photocathode it is possible to decrease or even elminate the external electrical potential [9].

Photovoltaic-electrochemical water splitting system is a combination of photovoltaics (PV) cell to convert solar energy into electricity and an electrolyzer to convert the electricity to chemical energy by splitting water into hydrogen and oxygen. Various types of electrolyzers are explained in Section 1.2. The main advantages of this system is that both PV cells and electrolyzers are technically developed and have already been commercialized. While the water splitting efficiency of electrolyzers is in the range of $60 - 83\%$, the efficiency of PV cells is almost 18% restricting the total efficiency of photovoltaic-electrochemical water splitting systems. However, the solar-to-hydrogen (STH) conversion efficiency of these systems is higher than 10% which is high enough to be economically viable [69].

1.6. Summary

For the given classification based on the driven energy, some recent publications regarding various hydrogen production methods are summarized in Table 1.1. Key features of literature and the main results, including the reached efficiency or STH, are mentioned.

Hydrogen production method	Short description of the project	Results	Date	Ref.
Thermolysis	Experimental direct thermolysis of water using concentrated solar radiation	$\eta = 1.17\%$	1986	[70]
	Experimental direct thermolysis of water within a solar furnace	$\eta = 1.1\%$	1983	[71]
Thermochamical water splitting	Thermodynamic performance assessment of solar based Sulfur-Iodine thermochemical cycle	$\eta_{I,cycle} = 43.85\%$, and $\eta_{I,sys} = 32.76\%$	2017	[17]
	Thermodynamic performance assessment of solar based Copper-Chlorine thermochemical cycle in presence of phase change materials	$\eta_{I,sys} = 80\%$, and $STF = 25.8\%$	2022	[72]
	Thermodynamic and economic assessment of solar based Copper-Chlorine thermochemical cycle	$\eta_{I,cycle} = 40.4\%$, and $\eta_{I,sys} = 28.77\%$, with hydrogen production capacity 1530.4 [kg/h]	2022	[73]

	Thermodynamic performance assessment of solar based ZnO/Zn thermochemical cycle	$STF = 62.6\%$	2021	[74]
	Thermodynamic performance assessment of solar based ZnO/ZnSO4 thermochemical cycle	$\eta_{I,cycle} = 40.6\%$ and $STF = 48.9\%$	2017	[75]
	Thermodynamic performance assessment of solar based SnO2/SnO thermochemical cycle	$\eta_{I,cycle} = 41.17\%$ and $STF = 49.61\%$ %	2017	[76]
Biomass gasification	Extensive set of small-scale biomass gasification systems available in European market is monitored on-site.	The most efficient technology has $\eta = 78.5\%$ with more than 20% molar fraction of hydrogen within the product gas.	2021	[77]
Coal gasification	Catalytic steam gasification of coal to produce hydrogen	Up to 61% hydrogen content within the product gases	2018	[78]
Steam methane reforming	Six different process arrangements for sorption enhanced steam methane reforming are proposed	Near 100% carbon capture with $\eta_{max} = 76.3\%$.	2020	[79]
Electrolysis	A review of AWE powered by renewable energy	$\eta_{stack} = 70\%$ for both AWE and PEM technologies.	2020	[80]
	Comparative study of AWE, PEM water electrolysis and SOE with the aid of multiphysics modeling	η_{PTH} of 50-60%, 65-70%, and 90-95% for AWE, PEM, and SOE water electrolysis	2022	[81]
	Performance and stability analysis of AEM without critical raw materials	$\eta = 80\%$ for the steady state condition.	2022	[82]
	A study of hydrogen production by electrolysis including fundamentals, engineering aspects and more detail description.	η = 51-60%, 46-60%, and 76-81% for AWE, PEM, and SOE water electrolysis	2020	[83]
	AEM water electrolysis with non-noble metal catalysts	$\eta = 75\%$	2020	[84]
	Anion exchange membrane alkaline seawater electrolysis with Ni-doped FeOOH anode	$\eta = 76.35\%$	2021	[85]
Photocatalysis	TiO2 photocatalytic hydrogen production enhanced with NiSe2 nanoparticles as a co-catalyst	$STH = 9\%$	2022	[86]
	A quadruple-band metal–nitride nanowire artificial photosynthesis system for photocatalytic solar water splitting	$STH = 5.2\%$	2019	[87]
	Visible light-driven water splitting using p-type metal-nitride nanowire arrays	$STH = 1.8\%$	2015	[88]

Biohydrogen	A coupled method of microalgae photosynthesis and dark fermentation to produce hydrogen	$\eta = 11.76\%$	2022	[89]
	Effects of temperature and total solid content on biohydrogen production from dark fermentation of rice straw is investigated.	The highest biohydrogen production is measured to be 63.60 ± 2.98 [mL/g].	2022	[90]
	Photo-fermentation biohydrogen production from corn stalk is enhanced by using iron ions.	The maximum hydrogen yield is increased 19.98% and reached 70.25 [mL/g] in comparison with the case without iron ions.	2022	[91]
	A review of green technology for sustainable biohydrogen production	$\eta_{max} = 2.6\%$ of light conversion is reported for the direct biophotolysis.	2020	[92]
Photovoltaic-electrolysis	Solar water electrolysis by photovoltaic-electrolysis in which two polymer electrolyte membrane electrolyzers are connected to the solar cell.	$STH_{average} = 30\%$ for 48 [h].	2016	[93]
Photoelectrochemical water splitting	Analysis of the optimal band gaps of light absorbers in integrated tandem photoelectrochemical water-splitting systems.	Light-absorbing materials with 1.6–1.8 [eV] band gap integrated with Si can have water splitting efficiencies more than 25%.	2013	[94]

Table 1.1: Summary of almost recent hydrogen production publications. $\eta_{I,cycle}$ is the first law efficiency of the cycle, $\eta_{I,sys}$ is the first law efficiency of the system, STF is solar-to-fuel conversion efficiency, η_{stack} is the nominal stack efficiency, η_{PTH} is power-to-hydrogen efficiency, and STH is the solar-to-hydrogen conversion efficiency.

2 | Photocatalytic hydrogen production

Photocatalytic solar to hydrogen conversion is a promising method to produce green and sustainable energy. Since the pioneering work of employing TiO_2 as the photocatalyst by Fujishima and Honda [95], various photocatalysts including inorganic semiconductors as well as conjugated polymeric photocatalysts have been introduced to drive the non-spontaneous water splitting reaction. As mentioned in Section 1.3, photosensitive semiconductors can be used as photocatalysts to decompose the water and thereby produce hydrogen. Semiconductors with suitable conduction band (CB) and valance band (VB) energy levels besides good separation of generated electron-hole pairs are the most efficient ones [13].

Photocatalytic materials can be classified based on their chemical composition into simple binary metal oxides and sulfides, multicomponent materials, nonmetal semiconductors, magnetic composites and metal organic frameworks (MOFs) [55]. Apart from the photocatalytic activity, stability, cost and toxicity, the light absorption range must also be considered to design a photocatalytic system with higher STH conversion efficiency. For instance, extensively studied TiO_2 photocatalyst is capable to absorb only UV light [60, 96], which is approximately 6% of the total electromagnetic solar spectrum.

2.1. Metal Oxides

Metal oxides consist of metal cations and oxygen anions have already been developed as heterogeneous catalysts for applications such as petrochemical industry. Metal oxides like oxides of titanium, vanadium, and zinc possess desired band gaps, stability, reusability, and light absorption ability making them suitable heterogeneous photocatalysts. A charge separation process (i.e. generation of electron-hole pair) occurs within these metal oxides when they are exposed to either ultraviolet light, visible light or a combination of both. The generated electron-hole pairs are capable to reduce and/or oxidize a compound which is adsorbed on the surface of the photocatalyst [97].

Since 1972 that Fujishima and Honda [95] used TiO_2 as a photocatalyst, it has been widely used to produce hydrogen [98]. However, the high recombination rate of generated electron-hole pairs has kept its efficiency low. Coupling TiO_2 with other semiconductors has been proposed as a way to decrease the recombination rate thereby improving the photocatalytic efficiency which will discussed in Section 2.3.

Pure water splitting with the aim of artificial photocatalytic hydrogen production has attracted a great deal of attention. However, utilizing the seawater to produce hydrogen would be more practical and cost effective. Recently, Zhang et al. [99] have investigated hydrogen production from seawater splitting under full solar spectrum in the presence of TiO_2 nanoparticles without any sacrificial agent. They have used three various crystal structures of TiO_2 nanoparticles, i.e. brookite, anatase, and rutile, as photocatalysts. They have reported the maximum hydrogen production rate of 1476 [μmol/g/h] for brookite TiO_2 which has shown outstanding photoelectric properties besides more suitable band gap position and consequently higher efficiency and stability in comparison with the other two structures. Moreover, they have reported that the hydrogen production rate by the brookite TiO_2 nanoparticles is higher for seawater than that in deionized water.

2.2. Metal sulfides

Metal sulfides consisting sulfur and a metal as the anion and cation respectively, are another group of promising semiconductors with photocatalytic properties. Owing to suitable electronic band position (i.e. shallow valence band), suitable band gap, exposed active sites, good catalytic activity, availability in various sizes and shapes, chemical compositions and excellent light response, metal sulfides are known as outstanding photocatalysts to harvest the total solar light spectrum [100].

Metal sulfides can be in the form of mono-metal sulfides (e.g., MoS_2, FeS, ZnS), bio-metal sulfides (such as $CuSbS_2$) or tri-metal sulfides (like $PbFeSb_6S_{14}$). Although the mono-metal sulfide MoS_2 is stable and has remarkable light absorption and excellent electronic arrangement, the indirect band gap of 1.2 [eV] in its bulk phase is inappropriate for the separation of charge carriers and consequently to start off the photocatalytic reaction. It has been revealed that using different morphology is a way to address this issue by customizing the band gap [100]. When the size of the MoS_2 is decreased to the two-dimensional scale like nanosheets, the indirect band gap is changed to a direct band gap of 1.9 [eV] which makes it a promising photocatalyst operating with visible light. Hence, various thicknesses of MoS_2 can be used as co-catalysts with other photocatalysts to improve the efficiency [101].

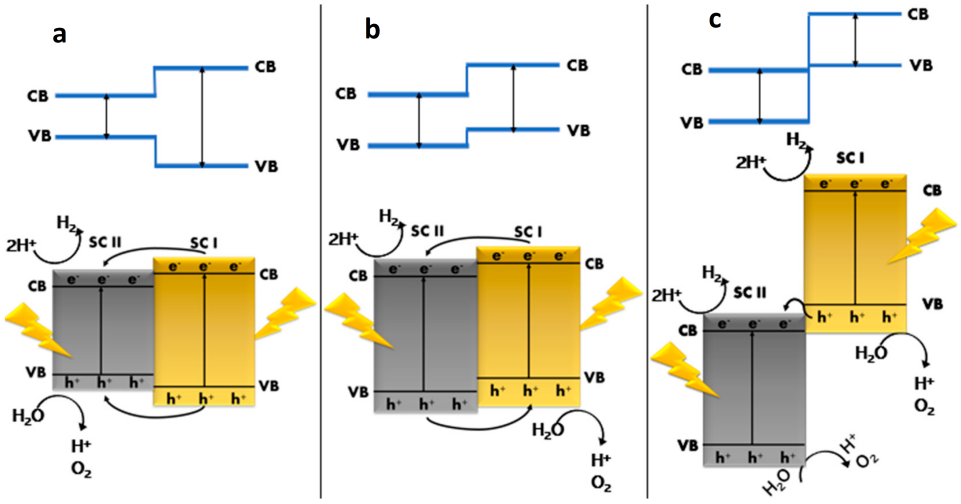

Figure 2.1: Schematic diagram of various heterojunctions, (a) type-I, (b) type-II and (c) type-III. Reproduced with permission from reference [102]

2.3. Multicomponent Materials

While the charge transfer is quite straightforward in previous materials, in multicomponent materials which is usually made of three different components forming a heterojunction system, the electron-hole pair recombination is delayed due to the fact that the charge passes through a buffer medium in its path between the heterosites. It is worthwhile to mention that the interface of the two components A and B can be considered as the nanojunction bridge and consequently forming a ternary system. Combination of semiconductors effects the surface structure as well as charge transfer characteristics of the resulting photocatalytic system making it possible to absorb a broader spectrum of light. Different types of possible heterojunctions are depicted in Figure 2.1.

As can be seen in Figure 2.1a, in type-I heterojunctions, the VB and CB of the semiconductor with smaller band gap is enclosed by those of the one with bigger band gap. In this type, generated electrons and holes can move from semiconductor I to semiconductor II. However, in type-II (see Figure 2.1b), both CB and VB of semiconductor II are below the CB and VB of the other one. Therefore, electrons move from conduction band (CB) of one component to CB of the other one, while holes migrate between the valance bands (VB) of components. In type-III of the heterojunctions, CB of one semiconductor is below the VB of the other one. For this type, electrons of semiconductor II will recombine with the holes on the semiconductor I. Among theses three types of heterojunctions, only type-II has the ability to enhance the fast spatial separation of generated electron holes that makes it the widely used heterojunction in photocatalysis. If the electrons of one

component recombine with the holes of the other one in a type-II heterojunction, electrons accumulate on one side and the holes move to the other side. It is known as direct Z-scheme heterojunction [102].

As mentioned in Section 2.1, TiO_2 has been exhaustively used as photocatalyst, even though, its photocatalytic activity is insufficient due to its high recombination of generated electron–hole pairs. So far, several investigations have been down on coupling of TiO_2 with different semiconductors to enhance it photocatalytic activity. Ramírez et al. [103] have studied core-shell structure of SnO_2/TiO_2 with different molar ratios. They figured out that the interaction between SnO_2 as the core and Tio_2 as the shell forms energetic states at the surface which enhances the separation of generated electron-holes.

Wang et al. [104] have investigated the photocatalytic water-splitting capability and STH conversion efficiencies of two crystal phase heterostructures (CPHS) including CdS/SPtSe (CPHS(S)) and CdS/SePtS (CPHS(Se)) by using hybrid density functional. They reported that negative interface formation energies besides the small lattice mismatches have made the CPHSs stable and feasible. Also, the narrow energy band gaps of the CPHSs make it possible to absorb adequate visible light. By switching the contact surface of the two semiconductors, the CPHSs flip between type-I and type-II without effecting the electronic structure. Type-I CPHS(Se)s have the potential to be employed as light-emitting diodes. The type-II CPHS(S)s band alignment promote photoinduced carriers' spatial separation, whereas the generated built-in electric field around the interface enhances separation and migration of photoexcited carriers. They revealed that the band edges of CPHS(S)s satisfy the thermodynamic criteria for photocatalytic water splitting, and STH conversion efficiency would be up to 37.5 percent. All their findings point out that the CPHS(S)s are highly efficient photocatalysts for water splitting.

In another study, a novel two-dimensional (2D) direct Z-scheme heterostructures photocatalyst based on $\beta-$GeSe and HfS_2 monolayers has been investigated by Liu et al. [105]. They took advantage of DFT theory to look into the potential photocatalytic properties as well as structural stability of the $\beta-GeSe/HfS_2$ heterostructure. It has been proved that the $\beta-GeSe/HfS_2$ heterostructure has an exceptional light absorption capability in a wide range including both ultraviolet and visible spectra. Furthermore, on the surface of this heterostructure and when pH is in the range of 7 to 12, the entire water splitting reaction proceeds spontaneously and concurrently without any additional overpotential or co-catalyst. With the $\beta-GeSe/HfS_2$ heterostructure they could reach the highest predicted STH efficiency of 37.95%.

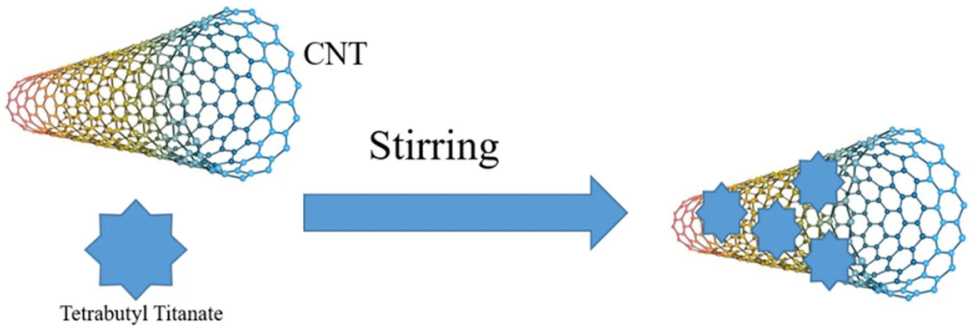

Figure 2.2: In situ growth of TiO_2 mesoporous composites on CNT. Reproduced with permission from reference [109].

2.4. Nonmetal Semiconductors

Graphitic carbon nitride (g-C_3N_4) is a novel nonmetal semiconductor which has gained considereable attention due to its narrow band gap, high thermal and chemical stability, availability of raw materials as well as its easy production in large-scale [106]. The g-C_3N_4-based materials such as its composites, mesoporous carbon nitride (mpg-C_3N_4) and its doped versions (with metal-free materials) are nonmetal semiconductor photocatalysts suitable for harvesting solar energy [107]. Apart from the suitable band gap (2.73 [eV]), large surface area and therefore more active sites of mpg-C_3N_4 make it more favorable catalyst in comparison with g-C_3N_4. However, mpg-C_3N_4 has lower quantum yield which shows lower efficiency of electron-hole pair generation that can be addressed by coupling it with another co-catalyst. In a study done by Liu et al. (2017), nitrogen-doped carbon nanotubes is used as the co-catalyst which has improved its photocatalytic activity [108].

In conjunction with metal oxides such as TiO_2, nonmetal semiconductors can be employed to enhance the photocatalyst's light harvesting capabilities. Currently, Bai et al. [109] have prepared a spot-coated carbon nanotube (CNT) composites by in-situ doping of carbon nanotubes into TiO_2 materials (see Figure 2.2) to produce catalysts with higher efficiency and stability. Besides lower degree of agglomeration, they have reported higher hydrogen evolution performance (0.0337 [mg/ml]) for the prepared nanocomposites.

Polymeric photocatalysts, particularly covalent triazine frameworks (CTFs), have shown to be a promising photocatalyst to produce hydrogen in the presence of light. Due to uniform distribution of donor–acceptor motifs within the structure of CTFs, the separation and transfer of charges are isotropic. Lan et al. [110] theoretically and experimentally have shown that the modification of the molecular structure of CTF-based photocatalysts by adding the electron donor thiophene (Th) or benzothiadiazole (BT) units (widely used electron donar and acceptor units, respectively) as the dopant leads to an anisotropic

charge carrier separation and migration. They have reported that the modified polymers have displayed a better photocatalytic activity to produce hydrogen in the presence of visible light. The hydrogen evolution rate under visible light irradiation ($\lambda > 420$ [nm]) for the pure CTF is reported to be 45 [μmol/h], while it is 62 and 112 [μmol/h] for CTF modified by Th and BT units.

2.5. Magnetic Composites

One of the most important applications of photocatalysts is water purification by degradation of organic pollutants. In this study we have focused on the hydrogen production so we have not mentioned water purification so far. However, in order to cover all possible photocatalytic materials, it is necessary to discus about it in this section. When a photon of light excites the photocatalyst and a pair of electron-hole is generated, the photoinduced hole (h^+) with sufficient energy oxidises the water molecule on the surface of the semiconductor through the following reaction:

$$H_2O + h^+ \longrightarrow OH^\bullet + H^+ \tag{2.1}$$

Then, the organic pollutants are oxidised in the presence of the oxidants i.e. electrons, holes, H^+, $OH^\bullet$, and even $O_2^\bullet$ [111].

For heterogeneous photocatalysts suspended within the polluted water, the efficient recovery is of importance. Magnetic materials are considered as a possibility in the isolation of heterogeneously catalyzed liquid-phase reactions. This fast, inexpensive and easy catalyst recovery is much efficient in nano-based catalysts because of their extremely small sizes which make effective separation very difficult by centrifuging at high speed. Generally, magnetic composites are consist of a magnetic core (magnetic materials like iron, nickel, cobalt as well as their oxides) and a shell made of a well known photocatalytic material (e.g., TiO_2 and ZnO). Jing et al. [112] have investigated a magnetic composite consist of Fe_3O_4 and TiO_2 as the magnetic core and photocatalytic shell, respectively. They have reported 90% of removal of pollutant within two hours while being irradiated by UV radiation. After three cycles, photodegradation of 84% is observed which is around 95% of the initial photocatalytic activity. In another study done by Chen et al. [113], recyclable cobalt nanocatalyst, supported on magnetic carbon with core-shell structure, is synthesized and used in hydrolysis of $NaBH_4$ at room temperature. They have reported the 1403 [$ml_{H_2}.g_{cat}^{-1}.min^{-1}$] hydrogen production rate.

Since the photocatalytic shell is in contact with the magnetic core, the main drawback

of this method is the probability of the core photo dissolution. It can lead to decrease in photocatalytic activity of the shell as well as change in the properties of the core. Therefore, in order to evade the direct electrical contact and consequently prevent the charge transfer between core and shell, an intermediate coating like SiO_2 is required. Besides the abovementioned features, SiO_2 is able to absorb light which can further enhance the photocatalytic performance of the whole composite. This magnetic composite configuration has demonstrated strong photocatalytic activity on the degradation of several organic compounds under UV and visible light [55].

2.6. Metal Organic Frameworks (MOFs)

Metal-organic frameworks (MOF) are porous materials with high porosity and specific surface area which are of interest due to their wide applications including gas separation/adsorption, organic transformations, carbon dioxide reduction, photocatalysis and hydrogenation. Cluster or metal ion nodes known as secondary building units (SBUs) besides organic linkers connecting the SBUs, and consequently making crystalline structures with significant porous texture development, are two components of the MOFs. Polytopic linkers like carboxylates, sulphates, phosphonates, and heterocyclic compounds are the widely used organic linkers. The combination of same SBU with various organic linkers leads to MOFs with different pore shapes thereby having different properties [114]. The main advantages of MOFs over conventional inorganic semiconductors are [115]:

- MOF's high porosity allows active areas to be exposed and catalyzed more easily.
- MOF's structural tunability makes it possible to adjust the light absorption range.
- Separation of electron-hole pairs are enhanced due to MOFs porous structure which leads to a short charge transfer path.
- It is also feasible to place co-catalysts or photosensitizers within the pores or on the framework to assist electron-hole pair separation.
- Tunability of structure of well-defined MOFs can be utilized to create a model to investigate the structure-activity relations.

In order to have a better photocatalytic activity, MOFs can be used in the presence of a co-catalyst. Zhou et al. [116] have studied a hybrid photocatalysts consists of UiO-66 metal organic framework and CdS as the co-catalyst. In comparison with UiO-66 and CdS alone, they have reported a significant improvement in hydrogen evolution activity of the developed hybrid system under the visible light irradiation. For the hybrid CdS

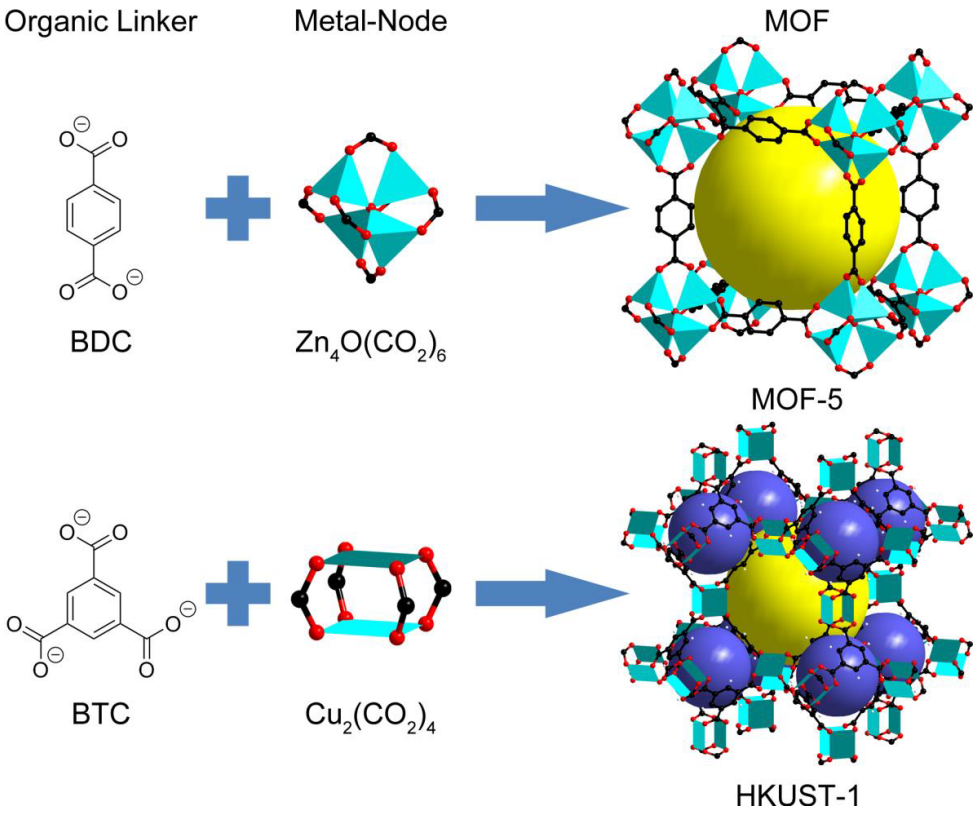

Figure 2.3: Schematic representation of secondary building units (SBUs) and organic linkers of MOF-5 and HKUST-1 metal organic frameworks. Yellow and blue spheres represent the free spaces. Reproduced with permission from reference [114].

/UiO-66, maximum 235 [μmol/h] of hydrogen production was reached. The efficient interfacial charge transfer between UiO-66 and CdS, which inhibits the recombination of the generated electron-hole pairs and consequently improves the photocatalytic activity, is attributed to the increased hydrogen production over this hybrid system.

2.7. Low dimensional materials

Since 2004 that Nan et al. [117] discovered the graphene, considering the many unique features arising from the bulk to monolayer transition, two-dimensional materials have been gaining popularity. For instance, the indirect band gap of 1.2 [eV] of MoS_2 in its bulk phase is changed to a direct band gap of 1.9 [eV] in its two-dimensional form of nanosheets [101]. Among the 2D family, the monolayer transition metal dichalcogenides (TMDs) are considered as the most promising cost efficient instead of noble metals as catalysts for hydrogen production. Pan et al. [118] have used the first-principles calculations so as to analyse the electrical and catalytic properties of Janus bismuth oxyhalide (Bi_2O_2XY in which X and Y are Cl, Br or I, and X$\neq$Y) for the hydrogen evolution reaction (HER). They have shown that Janus Bi_2O_2XY possesses a higher electron-hole pair separation efficiency and operates within a wider range of solar spectrum thanks to Janus asymmetry. Moreover, the asymmetric halogen surfaces on both sides generate an electrostatic potential difference, resulting in a staggered band alignment. They have found that, in comparison to BiOBr and BiOCl with 0.69% and 0.23% STH efficiency, Janus Bi_2O_2BrI and Bi_2O_2ClI have significantly higher efficiencies (corrected STH efficiency of 10.76% and 9.77% respectively).

3 | Energetic and Economical comparison

Hydrogen production technologies based on the fossil fuels benefits from well-established raw material infrastructures, developed production technologies, and being more cost competitive. Similarly, water electrolysis is also a well-developed hydrogen production method that makes use of current infrastructure and grid. In the short-term, these methods play a major part in the hydrogen market. Methane steam reforming and coal gasification with carbon capture, utilization, and storage besides biomass gasification can be classified as the mid-term approach [2]. On the other hand, to cover the demanded hydrogen in the long-term but with minimum global worming potential and environmental impact, low emission technologies including photoelectrochemical and photocatalytic water splitting, electrolysis using renewable electricity, nuclear and solar based thermochemical cycles, and biological methods will be of importance [14]. In this chapter we are going to compare hydrogen production via current water electrolysis technology connected to a PV with current photocatalytic water splitting method from technical and economic point of views. In order to have a better insight into these technologies, a case study is done for Oulu, Finland.

3.1. Energy assessment of Finland

Finland is located in northern Europe and is among the the world's most northern countries with a long and cold winters. As reported by IEA [1], during 2020, 32.4%, 23.4% and 20.3% of the total energy supply in Finland were produced by biofuels and wastes, oil, and nuclear energy sources, respectively (Figure 3.1). Almost two-thirds of Finland is covered by thick woodlands which is the reason behind why biofuels and wastes are the main energy sources. Figure 3.1 shows that, during last decade, energy supply from fossil fuel sources (i.e. oil and coal) has been reduced. But on the other hand, energy supply from wind and solar sources has been increased from 2015.

Figure 3.2 represents the electricity generation by solar energy in Finland. Despite of

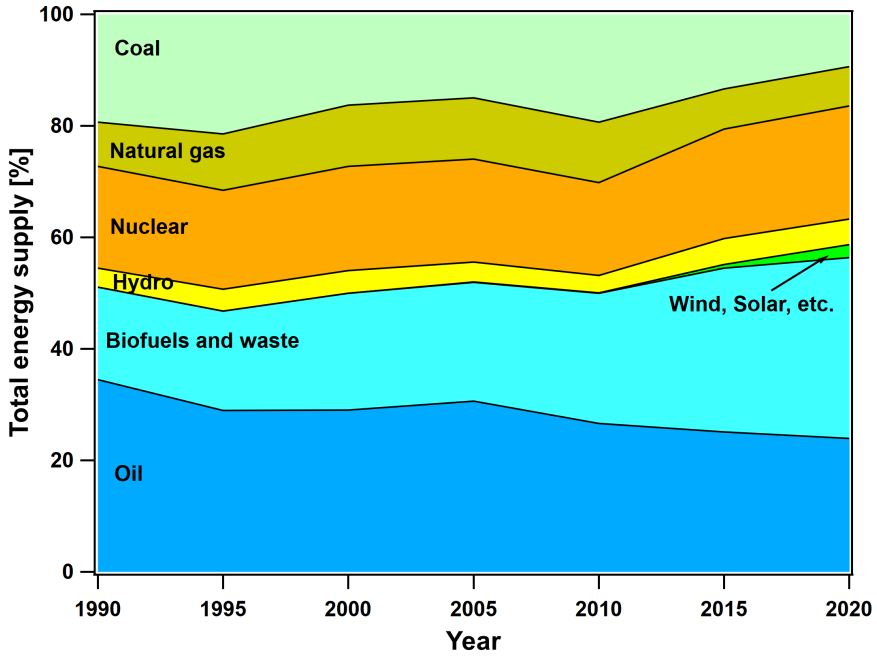

Figure 3.1: Total energy supply by sources for Finland [1]

the sharp increase in electricity generation by solar energy, still it is less than 0.5% of the total electricity generation (Table 3.1). Electricity generation via various sectors for Finland and Italy is tabulated in Table 3.1. As can be seen, nuclear and hydro powers are two major sectors for electricity generation in Finland, while natural gas and hydro are the major ones for Italy. Furthermore, solar energy share in electricity generation is 0.4% and 8.8% for Finland and Italy, respectively.

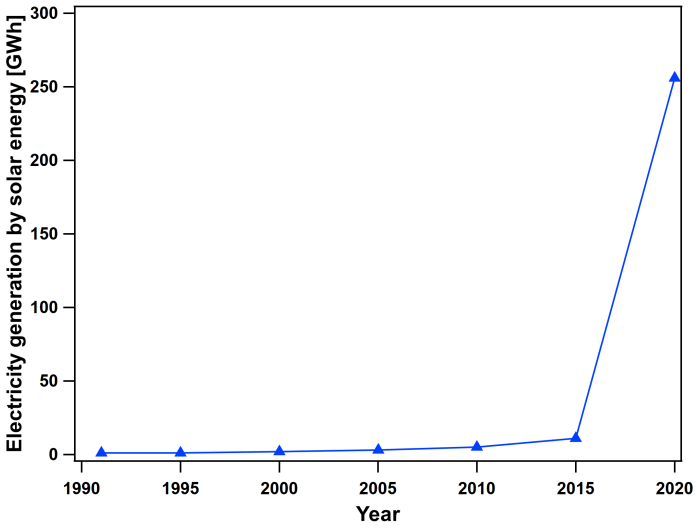

Figure 3.2: Electricity generation by solar energy for Finalnd [1]

Finland			Italy		
	GWh	%		GWh	%
Coal	5489	7.96	**Coal**	13064	4.64
Oil	266	0.39	**Oil**	9771	3.47
Natural gas	3702	5.37	**Natural gas**	137649	48.90
Biofuels	10996	15.95	**Biofuels**	17330	6.16
Nuclear	23291	33.78	**Geothermal**	6029	2.14
Hydro	15856	23.00	**Hydro**	48558	17.25
Solar PV	256	0.37	**Solar PV**	24942	8.86
Wind	7938	11.51	**Wind**	18702	6.64
Waste	892	1.29	**Waste**	4838	1.72
Other sources	260	0.38	**Other sources**	604	0.21
Total	68946	100.00	**Total**	281487	100.00

Table 3.1: Electricity generation by sector in 2020 for Finland and Italy [1]

3.2. Methods

3.2.1. PV plant with water electrolyser

In this section the utilized system and modelling procedure are described. The schematic diagram of the system which is considered to convert solar energy into hydrogen via PV

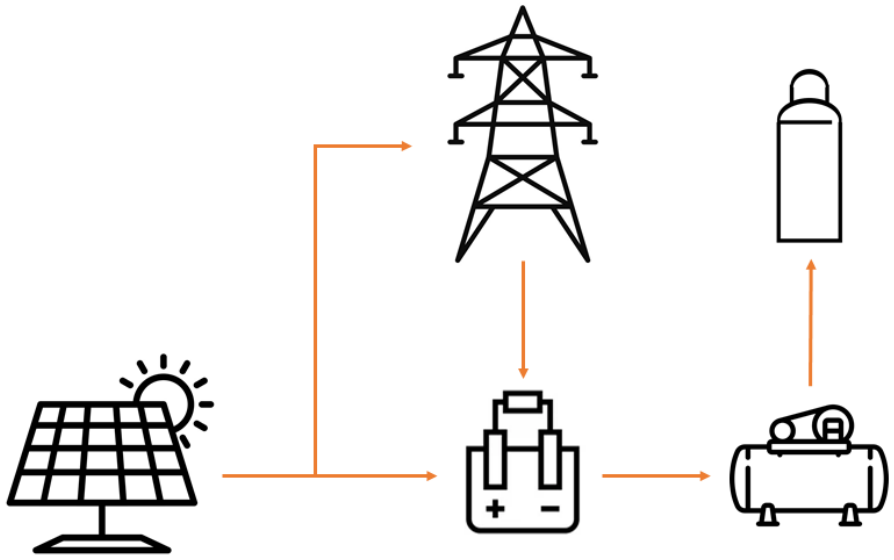

Figure 3.3: The schematic diagram of the proposed PV+EL system

plant is plotted in Figure 3.3. Here, the PV plant is connected to the grid and a Power-to-Gas (P2G) system consisting of a water electrolyser, and a pressurized hydrogen storage system (H_2 tanks). The considered elements are listed below:

- The PV plant including PV panels and the invertor to transform the DC current output of the panels to AC current.
- The electrolysis unit including purification system for the supply water, the separation tanks to separate production gases from water, a dryer for the supply water, and a transformer and rectifier in order to connect the system with the electric grid.
- The hydrogen storage unit including the hydrogen storage cylinders as well as a compressor pressurizing the produced hydrogen up to the cylinders maximum allowed pressure (i.e. 200 [bar]).

Despite the dark winters in high latitudes countries such as Finland, the long days during the summer can be worthwhile to invest on solar energy. Therefore, Oulu which is near Arctic Circle, has been selected as the location of the proposed system. In this study, the PV electricity generation data from Renewables.ninja (an online tool) for azimuth axis tracking with 58° tilt angle is used. In order to convert solar radiation data into power output, the Global Solar Energy Estimator model (GSEE) is utilized by this online tool [119, 120]. Figure 3.4 illustrates the average daily electricity generation ratio of PV to its peak capacity at Oulu in 2019. Since the electricity generation during November,

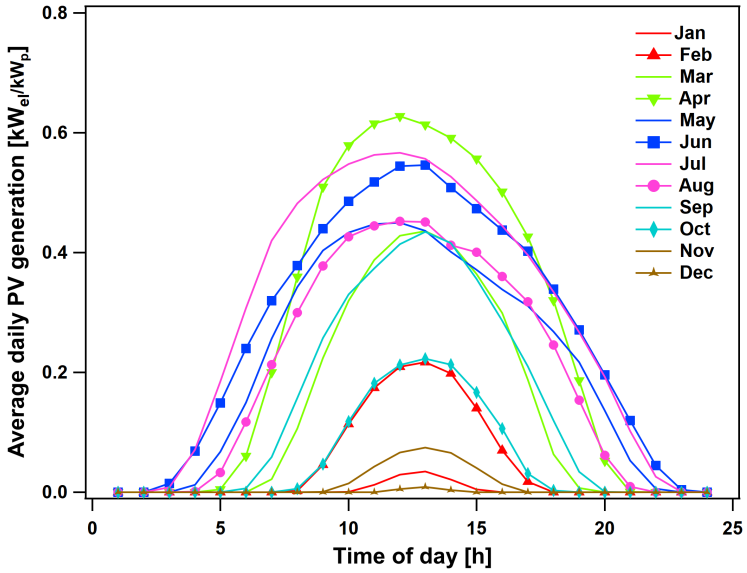

Figure 3.4: Average daily PV generation with respect to its peak capacity at Oulu in 2019 [120]

December and January is lower than 10% of the PV peak capacity, it is assumed that the proposed system operates only from the beginning of February to the end of October. Here, the year-long hourly time series in 2019 is considered for Oulu assuming it as a typical year profile (Figure 3.5a). Figure 3.5b shows the corresponding accumulated duration curve which is about 1200 equivalent operating hours (EOH).

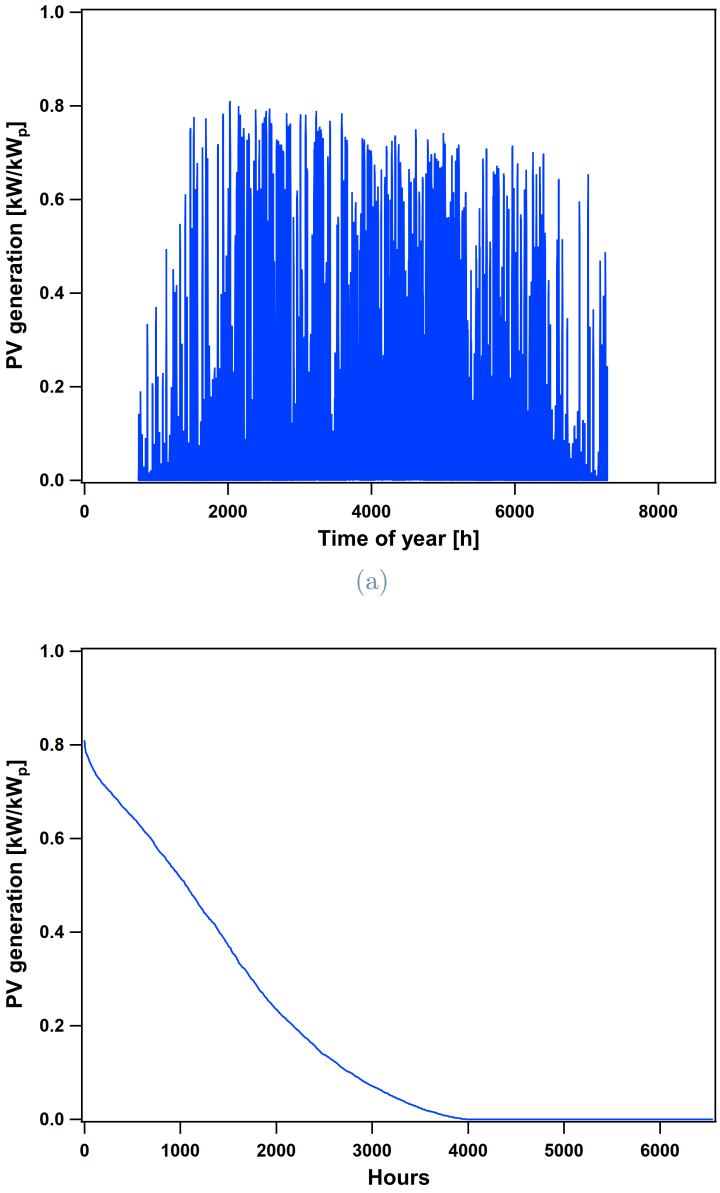

Figure 3.5: (a) Hourly PV generation with respect to its peak capacity, and (b) Solar PV generation duration curve in 2019 for Oulu, Finland [120].

Based on the proposed system, two different scenarios are selected to produce hydrogen:

- $S1$: when only the electricity from PV plant is used to produce hydrogen (green hydrogen)
- $S2$: Electricity from grid is utilized to run the electrolyser with at least its half capacity (as the first guess) when there is not enough electricity coming from the PV plant.

The electricity generated by the PV plant (E_{PV}) is divided into the portion used by water electrolyser (E_{PVtoEL}) and the one sent to the grid ($E_{PVtoGRID}$).

$$E_{PV}(t) = E_{PVtoEL}(t) + E_{PVtoGRID}(t) \tag{3.1}$$

When the generated electricity by PV is more than the electrolyser capacity, the excess electricity will be sent to the grid for both scenarios. However, for $S1$, when the generated electricity is lower then the minimum capacity of the electrolyser, it will be also sent to the grid. On the other hand, when the generated electricity is less than half of the electrolyser capacity, the remain electricity will be supplied by the grid in $S2$. Therefore, for hydrogen production the equation is:

$$E_{H_2,prod}(t) = (E_{PVtoEL}(t) + E_{GRIDtoEL}(t) - E_{comp}(t)) \times \eta_{EL} \tag{3.2}$$

in which, η_{EL} is the efficiency of the water electrolyser and E_{comp} is the consumed electricity by the compressor to pressurize the produced hydrogen.

By assuming a negligible leakage for the hydrogen storage tank, the energy stored in the form of H_2 gas and the energy consumed by the compressor will be:

$$E_{H_2,tank}(t+1) = E_{H_2,tank}(t) + E_{H_2,prod}(t) \tag{3.3}$$

and

$$E_{comp}(t) = \frac{E_{H_2,prod}(t)}{LHV_{H_2}} \times w_{comp} \tag{3.4}$$

here, w_{comp} is the specific consumption of the compressor and $LHV_{\mathrm{H_2}}$ is the lower heating value of the hydrogen gas. For a three-stage inter-cooled compressor that has constant compressor ratio on each stage with constant efficiency, w_{comp} will be 4 [MJ/$\mathrm{kg_{H_2}}$] when hydrogen gas is compressed from 30 [bar] to 200 [bar] [121].

For the first set of calculations Equations (3.1) to (3.4) is solved for both scenarios with the PV peak power of 1 [MW], and the electrolyser capacity of 400 [kW] (as the first guess) with 10 percentage minimum load. Figure 3.6 shows the integration between the PV generation and water electrolyser operation for this case. The technical information of the utilized components are shown in Table 3.2.

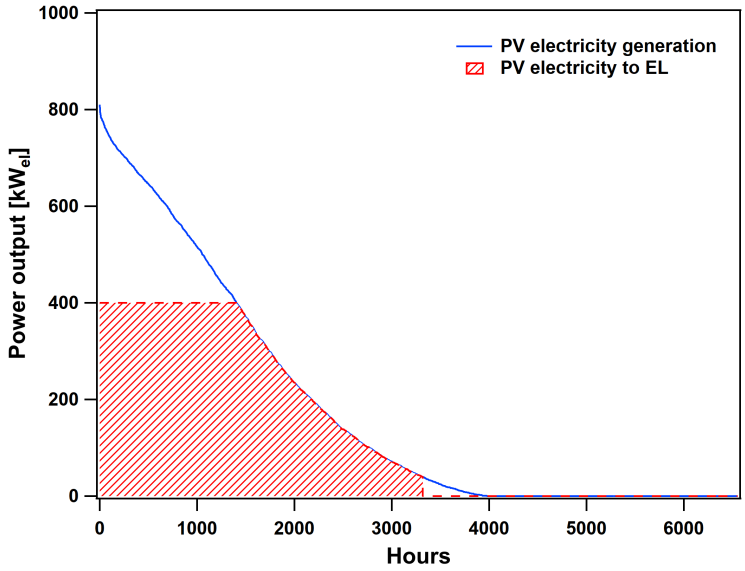

Figure 3.6: Integration between PV generation and EL operation.

Component	Type	Efficiency	Minimum load
PV	Monocrystalline Silicon with one axis tracking	20%	-
El	PEM electrolysis	70% (EE-to-LHV)	10%
H2 storage	200 bar cylinders	Negligible leakage	-
Compressor	Intercooled volumetric comp.	60-70%	-

Table 3.2: Technical parameters of components [121]

By taking all abovementioned assumptions into account and solving Equations (3.1) to (3.4), the hourly hydrogen production is calculated for both scenarios. As can be seen from Figure 3.7, when the electricity generation by PV is higher than the required electricity to operate the EL with its half capacity, both scenarios have same hydrogen production. When the produced electricity is lower than the minimum capacity of the EL, the electricity is sent to the grid for the first scenario (Figure 3.8). This is the reason behind the higher amount of the excess electricity for first scenario in comparison with the second one (Figure 3.9).

The economic assessment of the proposed system is developed in this section. To do this, the total investment cost (I_{CAPEX}) and the yearly maintenance prices ($I_{OPEX}(t)$) are calculated for all components, i.e., PV plant, water electrolyser, hydrogen storage unit, and the compressor. The list of the component prices are given in Table. 3.3. It is

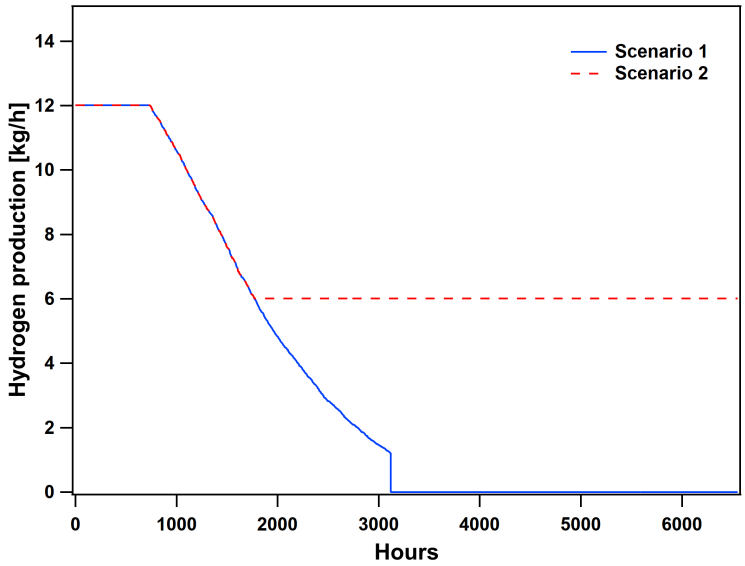

Figure 3.7: Hydrogen production [kg] for both scenarios (PV peak power of 1 [MW] and EL capacity of 400 [kW])

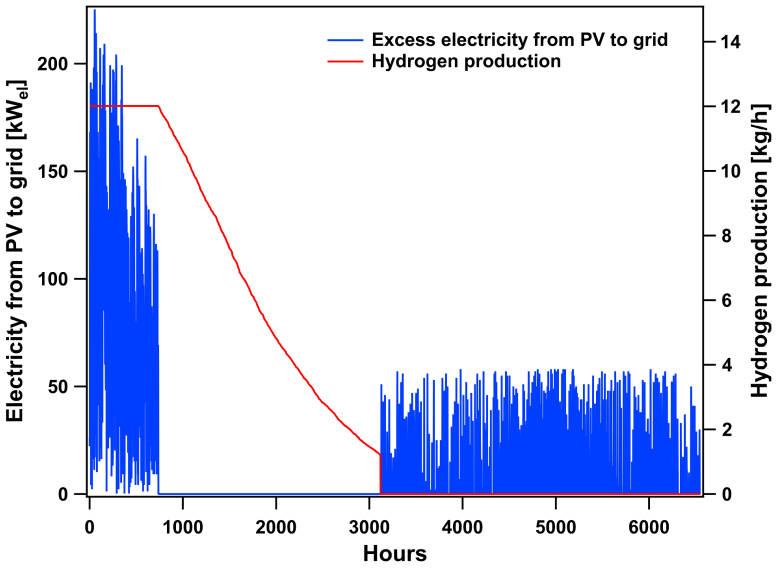

Figure 3.8: Excess electricity produced from PV to grid as well as produced hydrogen for Scenario 1

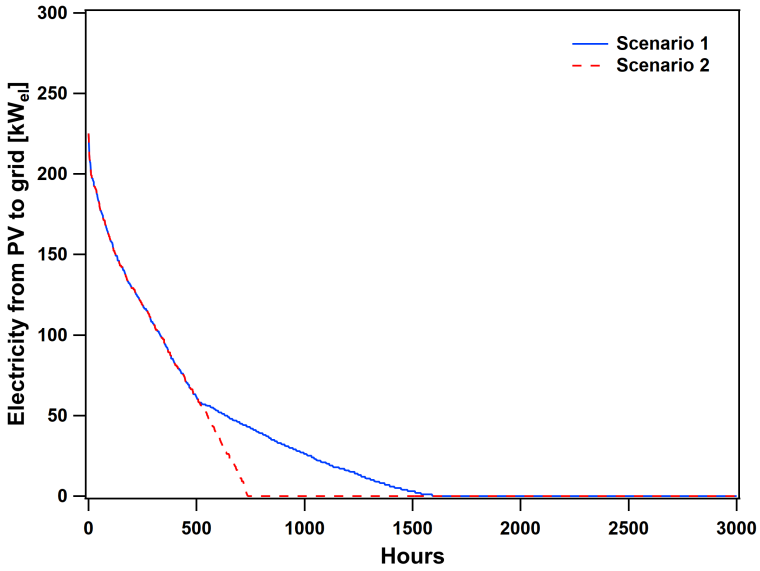

Figure 3.9: Excess electricity produced by PV and sent to grid

assumed that the investment is conducted in one installments which is defined 0 year in calculations which is amortized in 15 years equally.

$$I_{CAPEX} = \sum_i P_i \times CAPEX_i \tag{3.5}$$

$$I_{OPEX} = \sum_i P_i \times OPEX_i \tag{3.6}$$

here, P_i is the capacity of component i. In order to calculate the yearly revenue Equation (3.7) is used. C_{sell} is the price of the electricity which is sold to grid, and $C_{\mathrm{H_2}}$ and $m_{\mathrm{H_2}}$ is the price and mass of the produced hydrogen.

$$Revenues(t) = E_{PVtoGRID}(t) \times C_{sell} + m_{\mathrm{H_2}}(t) \times C_{\mathrm{H_2}} \tag{3.7}$$

By subtracting the yearly operation cost, amortization and the cost of the electricity from the grid for the $S2$, the yearly profit before tax is calculated (Equation (3.8)). In this study, 5 years tax exemption is assumed.

$$Profit(t) = Revenues(t) - I_{OPEX}(t) - Amort.(t) - E_{GRIDtoPV}(t) \times C_{purch} \tag{3.8}$$

By multiplying profits with the tax rate (T_t), yearly tax can be calculated (Equation

(3.9)). Here, five years of tax exemption has been assumed.

$$Tax(t) = Profit(t) \times T_t \tag{3.9}$$

For cash flow, discounted cash flow and cumulative cash flow, the below equations are used. Here, r represents the inflation rate.

$$CashFlow(t) = Revenues(t) - I_{CAPEX}(t) - I_{OPEX}(t) - Tax(t) \tag{3.10}$$

$$DisCash(t) = \frac{CashFlow(t)}{(1+r)^t} \tag{3.11}$$

$$CumCash(t) = CumCash(t-1) + DisCash(t) \tag{3.12}$$

All parameters required for economical assessment are listed in Tables. 3.3 and 3.4.

Component	CAPEX	OPEX	Ref.
PV	946.08 [€/kWp]	1.28 % of CAPEX [€/year]	[122]
El	1185 [€/kWel]	2 % of CAPEX [€/year]	[121]
H2 storage	1600 [€/kWel]	1 % of CAPEX [€/year]	[121]
Compressor	500 [€/kg]	1 % of CAPEX [€/year]	[121]

Table 3.3: CAPEX and OPEX of the component

Parameter	Value	Ref
Lifetime	25 years	-
Interest rate	5.4%	[123]
Inflation rate	2.2%	[124]
Tax rate	20%	[123]
Tax exemption	5 years	-
Financial amortization	15 years	-
Electricity purchase price	7.77 [c/kWh]	[125]
Electricity Sell price	4.27 [c/kWh]	[126]

Table 3.4: Assumptions for the economical assessments for Oulu, Finland

The capacity of the electrolysis unit is of importance for the proposed system. Therefore,

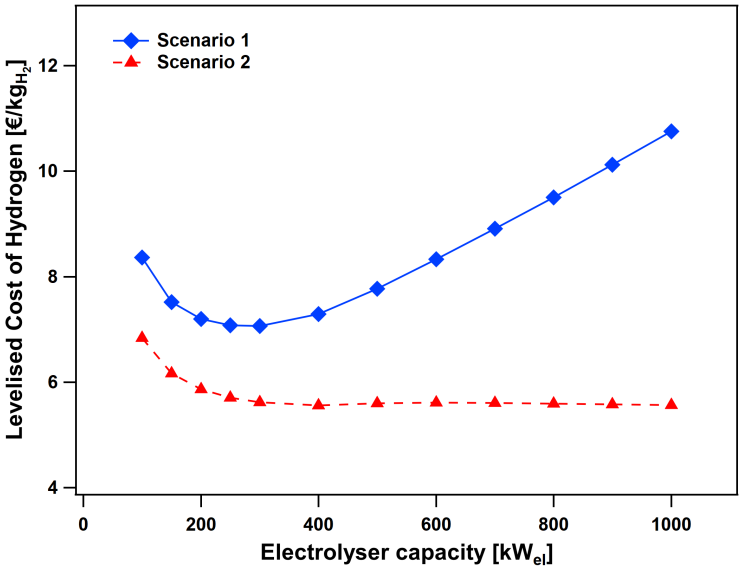

Figure 3.10: Levelised Cost of Hydrogen [€/kg$_{H_2}$]

for both scenarios, Levelised Cost of Hydrogen (LCOH) has been calculated for various water electrolyser capacity to find the optimal system for the given PV capacity. LCOH is the price of hydrogen that covers all the investment and operating costs of the system without profit which makes the cumulative cash flow for the last operation year to be equal to zero.

As depicted in Figure 3.10, LCOH for $S1$ is always higher than $S2$ which shows that the price of the green hydrogen will be higher. For the current system, with hydrogen storage capacity for 4 days, the optimal capacity of electrolysis unit for green hydrogen production is $250-300$ [kWel]. For the second scenario, by increasing the capacity of water electrolyser, LCOH is almost constant showing that the price of the produced hydrogen will depend mainly on the price of the electricity. Because, for higher EL/PV power ratios capacities, the electricity from the grid is the main source of energy to produce hydrogen.

Component	CAPEX [€]	CAPEX [%]
PV	946080	56.46
El	355500	21.22
H2 storage	356357	21.27
Compressor	17618	1.05

Table 3.5: Investment cost of each component for PV peak power of 1 [MW], EL capacity of 300 [kW], and 4 days hydrogen storage capacity

Table. 3.5 shows the capital cost of each component for the system with PV peak power of 1 [MW], and EL capacity of 300 [kW] which has the capacity to store maximum 4 days of produced hydrogen. As can be seen, the hydrogen storage unit cost is comparable with even PV panels. The cost of the storage unit will be equal to the PV plant cost for approximately 10 days hydrogen storage capacity.

To have a better insight into the proposed system, whole calculations are repeated for Milan. The PV electricity generation data from the same source is considered with same technical parameters. However, for the economic assessment of the system, different parameters are used which are given in Table. 3.6. Although the hardware costs for PV facilities is same for both countries, the soft costs (including, the cost of relevant permits, marketing, sales and administrative costs) and installation costs are lower in Italy leading to lower CAPEX of 826.15 [€/kWp] [122].

Parameter	Value	Ref
Lifetime	25 years	-
Interest rate	6.69%	[123]
Inflation rate	2.2%	Similar to Finland
Tax rate	24%	[123]
Tax exemption	5 years	-
Financial amortization	15 years	-
Electricity purchase price	16.47 [c/kWh]	[121]
Electricity Sell price	9.00 [c/kWh]	[127]

Table 3.6: Assumptions for the economical assessments of the system for Milan, Italy

Figure 3.11 illustrates the LCOH for both locations, i.e. Oulu and Milan. For electrolyser capacity bigger than 300 [kWel], the LCOH for $S1$ for Milan has an increasing trend similar to the one for Oulu. For the second scenario, the LCOH has lower slope for both locations. On the other hand, for electrolyser capacity of less than 300 [kWel], both scenarios for Milan have shown a completely different trend. This different behaviour is due to the difference in the sell and purchase price of the electricity which are more than twice bigger than those for Oulu. It is also clear form figure that the LCOH of green hydrogen in Milan is lower than Oulu, however, it is higher for Milan for $S2$ with electrolyser capacity approximately more than 200 [kWel].

Figure 3.12 represents the green hydrogen production for both locations for the PV peak power of 1 [MW], and EL capacity of 400 [kW]. As it is clear from the figure, the amount

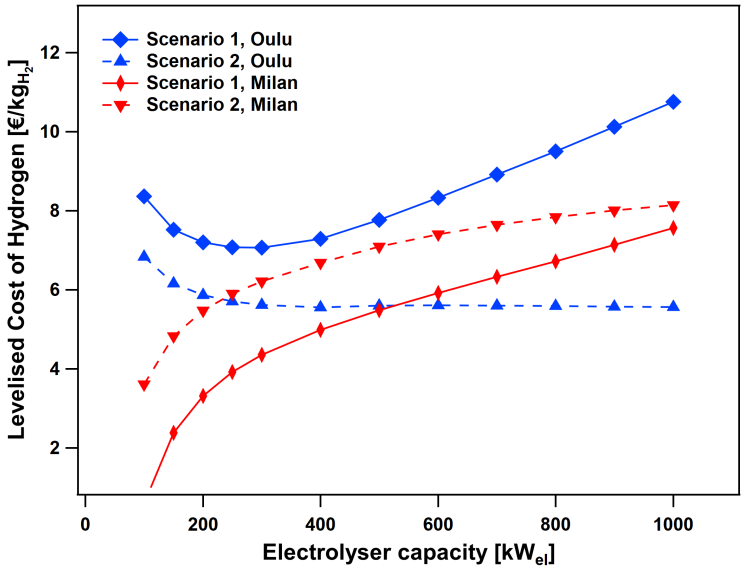

Figure 3.11: Levelised Cost of Hydrogen [€/kg$_{H_2}$] for Oulu and Milan

of the produced hydrogen is higher for Milan due to higher solar radiation.

Figure 3.13 illustrates the effect of the minimum electrolysis capacity that should be met with electricity by PV plant or the grid (for the second scenario). It shows that by increasing the percentage of the minimum electrolysis capacity from 25% to 75%, LCOH reduces for Oulu. However, LCOH is increased for Milan by increasing the minimum electrolysis capacity. This contradiction is due to the difference in the electricity price for considered locations. The low electricity price for Oulu leads to cheaper hydrogen production while the high electricity price in Milan makes it more expensive.

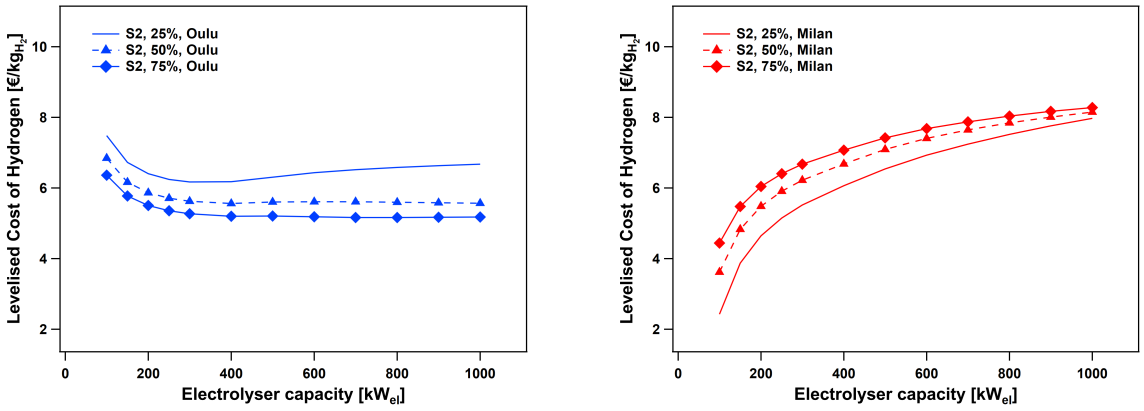

(a) (b)

Figure 3.13: LCOH for $S2$ with various minimum electrolysis capacity for a) Oulu, and b) Milan

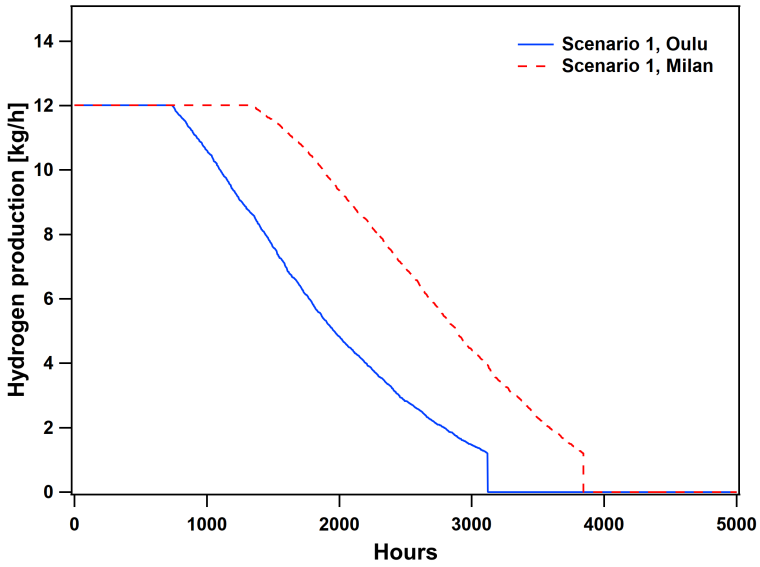

Figure 3.12: Green hydrogen production comparison between Oulu and Milan

3.2.2. Photocatalysis

In order to compare the proposed PV+EL system with photocatalytic method, STH (solar-to-hydrogen) conversion efficiency is employed. STH is defined as the ratio of out put energy in the form of hydrogen gas to the input energy of the incident solar light for any time intervals.

$$STH(\%) = \frac{r_{H_2} \times \Delta G_{H_2O}}{I_{solar} \times A} \times 100 \tag{3.13}$$

Here, $r_{\mathrm{H_2}}$ is the hydrogen evolution rate in [mol/s], $\Delta G_{\mathrm{H_2O}}$ is the Gibbs free energy change for the generation of one mole of hydrogen by splitting water under standard conditions (237.2 [kJ/mol]), I_{solar} is the light energy flux in [kW/m^2] and A represents the irradiation area in [m^2] [128, 129].

Figure 3.14 represents the STH efficiency of the PV+EL system for the first operating year in both locations (9 months operation for Oulu and 12 months operation for Milan). Due to the uncertainty in assumptions, the two are almost identical. Even though, the efficiencies of the PV panels and water electrolysis unit are constant, the STH conversion efficiency varies by the electrolyser capacity. Because, by increasing the capacity of electrolysis unit, the proposed system is able to produce more hydrogen from the same amount of the available solar radiation (i.e., same produced electricity by PV) and consequently it will have higher STH efficiency.

The maximum theoretical STH for the proposed system would be: $\eta_{PV} \times \eta_{EL} = 14\%$. However, the maximum STH efficiencies for Oulu and Milan are calculated as 13.03% and

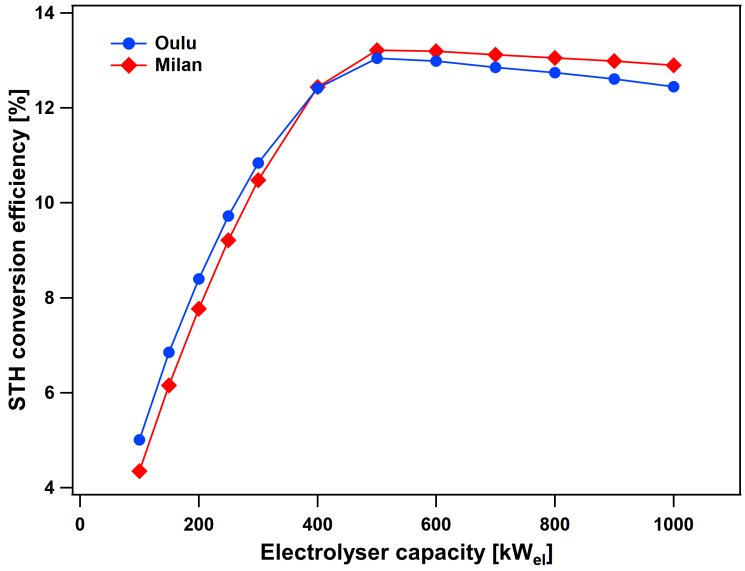

Figure 3.14: Solar-to-hydrogen conversion efficiency of proposed PV+EL system for Oulu and Milan

13.21% respectively, for electrolyser capacity of 500 [kWel] (Figure 3.14). For this case, almost 66.5% ($\eta_{EL} = 70\%$) of the generated electricity is stored in the form of hydrogen gas and 2.9% of it is sold to grid. Therefore, the current system is capable to convert almost 13.86% of the solar radiation to hydrogen and electricity. The water electrolysis unit with capacity of 500 [kWel] is the saturation point of the available power for this system. For electrolysis capacity higher than 500 [kWel], the amount of the available solar energy decreases due to the fact that the minimum load increases. It is interesting that despite the difference in sun availability, the optimal power ratio remain the same.

Since the photocatalytic water splitting method directly converts solar energy into hydrogen, it is possible to reach higher efficiency comparing to the PV+EL system. It could be more interesting to compare the amount and cost of the produced hydrogen via these two methods for the same area at the same location. Unfortunately, due to the lack of detailed technical information, it is not possible. However, to have a better understanding, for a particular photocatalyst, the investment cost is calculated based on the minimum reported LCOH by the considered PV+EL system for Oulu. The schematic diagram of the proposed photocatalysis water splitting unit is depicted in Figure 3.15.

A quadruple-band metal–nitride nanowire photocatalyst is designed and synthesised by Wang et al. [87]. These multi-band nanowires have energy band gaps of $\sim$ 2.1 [eV], 2.4 [eV], 2.6 [eV], and 3.4 [eV] which enable them to absorb wider range of solar spectrum. The STH conversion efficiency of 5.2% is reported for water splitting for this photocatalyst. To

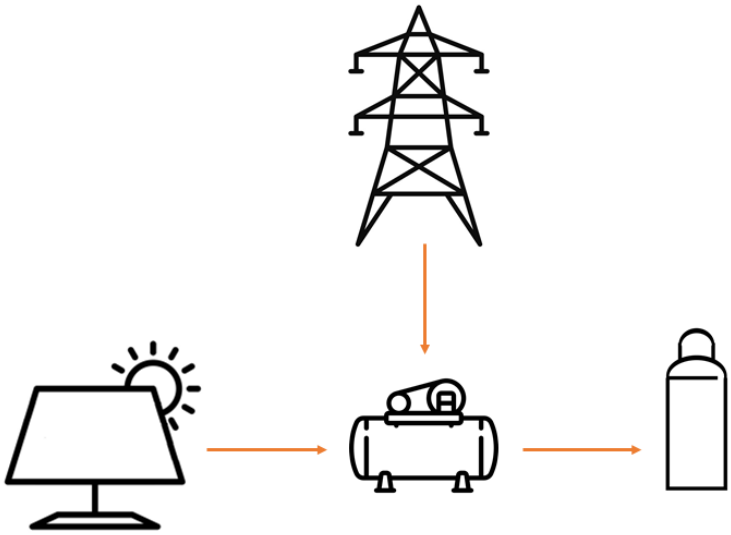

Figure 3.15: The schematic diagram of the proposed photocatalysis water splitting unit.

calculate the investment cost of the photocatalytic water splitting unit, it is assumed that multi-band nanowires are synthesised over the suitable panels which have the same area of the PV panels used in PV+EL system. The produced hydrogen gas will be compressed and stored within the storage tanks which has the capacity to store the produced hydrogen during 4 days, similar to the previous system. By considering the $STH = 5.2\%$, and the same solar irradiation, the hourly hydrogen production is calculated using Equation (3.13). Almost 9500 [kg] hydrogen is produced with considered assumptions which is 48% of the produced hydrogen by the PV+EL system.

For economic analysis, same price of the electricity is taken into account for the electricity required by the compressor (Table 3.4). It is assumed that the yearly operation cost of the photocatalytic panels is 2% of its CAPEX. Same values of PV+EL system are considered for the remaining parameters, including CAPEX and OPEX of compressor and storage tank. For the minimum calculated LCOH by PV+EL system for Oulu (i.e., 7.07 [€/kg]), the total investment cost of almost 0.68 [M€] is found, using Equations. (3.5) to (3.12). Therefore, for the photocatalytic water splitting to be economically comparable with PV+EL system, its total investment cost should be lower than 0.68 [M€]. The CAPEX of photocatalytic panels is around 0.5 [M€] which is near 39% of the CAPEX of both PV plant and water electrolysis unit. It should be mentioned that the compressor and hydrogen storage capacities will also lower in comparison to PV+EL system, which reduces the total CAPEX to 46%.

For the photocatalytic water splitting system producing the same amount of the hydrogen as PV+EL system, the total area of the photocatalytic panels should be 2.08 times of the PV panels area. In this case, the same LCOH is reachable by almost 87% of investment cost of the PV+EL system. In should be noted that the land cost is not considered which can affect this value. By considering abovementioned assumptions, the cost of 1 [m^2] photocatalytic panel (made of the quadruple-band metal–nitride nanowire photocatalyst) should be lower than 125 [€] to produce hydrogen with a price comparable with the PV+EL system.

The whole calculations has been repeated for same LCOH as well as the same total investment cost in order to find the corresponding STH conversion efficiency. The STH conversion efficiency of 12.45% is calculated based on the minimum LCOH (7.07 [€/kg]) and related investment cost of the proposed PV+EL system. The calculated STH represents the minimum conversion efficiency that photocatalytic panels should have, to be economically comparable with the current PV+EL technology.

4 | Conclusions and future developments

4.1. Conclusions

Considering the daily increase in the total energy consumption all over the world and its impact in the environment, using cleaner sources of energy with lower greenhouse gases emission is of importance. Hydrogen is a clean fuel with a heating value more than twice of the methane which only produces water when it burns. Therefore, green hydrogen can be a promising alternatives to fossil fuels. The green hydrogen is referred to hydrogen produced by using renewable sources or nonrenewable ones with carbon capture, utilization and storage (CCUS) unit. Material source of hydrogen is also of importance to produce green hydrogen. Even though water is the most clean source to produce hydrogen, currently near 96% of hydrogen is derived from conventional fossil fuels.

The present hydrogen production methods can be divided in conventional and renewable methods which have been briefly explained in Chapter 1. Photocatalytic water splitting is one of solar-driven hydrogen production methods that transforms directly the solar energy into chemical energy in the form of hydrogen gas. Photocatalytic materials based on their chemical composition has been classified and explained in Chapter 2.

Finally, to compare the photocatalytic water splitting with the current solar-driven hydrogen production technology, a solar water splitting unit consisting of a photovoltaic plant, and a water electrolysis is developed in Chapter 3. The proposed PL+EL system is studied for Oulu, Finland, and Milan, Italy. Two different scenarios are considered; only the electricity generated by PV is utilized to produce green hydrogen ($S1$), and electricity from grid is also used to run the electrolysis unit with its half capacity ($S2$).

As expected, the amount of the produced hydrogen for first scenario (green hydrogen) is higher for Milan due to higher available solar radiation in comparison with Oulu. Therefore, the levelized cost of hydrogen (LCOH) for both scenarios is higher in Oulu in comparison with Milan. While, the LCOH of $S1$ is higher in Oulu, the LCOH of $S2$ is

higher in Milan. Because of the huge difference in the electricity price between Finland and Milan making it more economical in Oulu to use the grid electricity to produce hydrogen. In Oulu, the minimum LCOH for $S1$ is calculated for water electrolysis capacity of 300 [kWel] and then by increasing the electrolysis capacity, LCOH also rise. On the other hand, the LCOH is roughly constant for higher electrolysers capacity for $S2$. However, by increasing the capacity of the electrolysis unit, LCOH increases for both scenarios but less sharply for second scenarios in Milan. By increasing the minimum electrolyser demand which should be met even with grid electricity for $S2$, the LCOH decreases for Oulu, while for Milan, conversely, it increases. It again highlights the importance of the purchase price and the sell price of the electricity for hydrogen production via PV+EL system.

Interestingly, the solar-to-hydrogen conversion efficiency is almost similar for both locations. Increasing the water electrolysis capacity improves the STH conversion efficiency sharply till it reaches its maximum value of approximately 13% for 500 [kWel] capacity. Then, increasing the electrolyser capacity does not effect the STH conversion efficiency noticeably.

A photocatalytic water splitting system made of quadruple-band metal–nitride nanowire photocatalyst with $STH = 5.2\%$ is compared with the proposed PV+EL system. For the photocatalytic panels covering the same area as PV panels, the minimum hydrogen production should be 48% of the PV+EL production so as to have the same minimum LCOH for Oulu (7.07 [€/kg]). In this case, the total investment cost is calculated to be 42% of the PV+EL system. In order to have the same hydrogen production with the same LCOH (7.07 [€/kg]), the area covered by the photocatalytic panels is found to be 2.08 times of the area covered by the PV panels. Without considering the land price, in this case, the total investment cost will be 87% of the PV+El system. These results demonstrate that the photocatalytic water splitting system should have lower investment costs in comparison with PV+EL system. Moreover, for the photocatalytic water splitting system with same LCOH and investment cost, STH conversion efficiency of 12.45% is calculated. Therefore, a photocatalytic water splitting system should have STH conversion efficiency higher than 12.45% to be economically comparable with the current PV+EL technology.

4.2. Future developments

In this study, hydrogen production using photocatalytic water splitting method is compared with the photovoltaic assisted water electrolysis method. Electricity is the energy

source of water electrolysis method. However, for proposed photocatalytic water splitting method, electricity is only required to compress the produced hydrogen gas which is less than 2% of the total electricity required for hydrogen production via water electrolysis. Moreover, considering the contradictory behaviour of the LCOH for Oulu and Milan, the importance of the purchase and sell prices of the electricity becomes more clear. Currently, the price of electricity has been increased and it is expected to rise even more. Furthermore, inflation rate is also an important factor affecting the LCOH which is also increasing. Therefore, the effect of the electricity price and inflation rate on the LCOH can be taken into consideration as the future development for current study.

More importantly, the lack of detailed information about the photocatalytic water splitting makes it challenging to do the comparison with current commercial hydrogen production methods. Usually, the hydrogen production rate for photocatalytic water splitting is reported in the form of $[\mu\text{mol.h}^{-1}.\text{g}_{\text{cat}}^{-1}]$ without reporting the density of the produced photocatalysts. Moreover, the intensity of utilized light is generally reported in [W] without giving information about the surface area that receives this power. The abovementioned parameters affects the technical assessment of the photocatalytic water splitting units. Even though a couple of large scale photocatalytic water splitting studies have been done so far, there is a big gap in economical information regarding this technique. In conclusion, studying the photocatalytic water splitting with more details, which can makes the comparison with other hydrogen production methods possible, can be considered as the developments for current study.

Bibliography

[1] IEA. Database documentation, electricity information, 2021 edition, 2022. URL https://www.iea.org/data-and-statistics.

[2] Ephraim Bonah Agyekum, Christabel Nutakor, Ahmed M. Agwa, and Salah Kamel. A critical review of renewable hydrogen production methods: Factors affecting their scale-up and its role in future energy generation. *Membranes*, 12(2), 2022. ISSN 2077-0375. doi: 10.3390/membranes12020173. URL https://www.mdpi.com/2077-0375/12/2/173.

[3] Alexandra M Oliveira, Rebecca R Beswick, and Yushan Yan. A green hydrogen economy for a renewable energy society. *Current Opinion in Chemical Engineering*, 33:100701, 2021.

[4] Tatiane da Silva Veras, Thiago Simonato Mozer, Aldara da Silva César, et al. Hydrogen: trends, production and characterization of the main process worldwide. *International journal of hydrogen energy*, 42(4):2018–2033, 2017.

[5] Pavlos Nikolaidis and Andreas Poullikkas. A comparative overview of hydrogen production processes. *Renewable and Sustainable Energy Reviews*, 67:597–611, 2017. ISSN 1364-0321. doi: https://doi.org/10.1016/j.rser.2016.09.044. URL https://www.sciencedirect.com/science/article/pii/S1364032116305366.

[6] A.E. Mazraeh, M. Babayan, M. Yari, Ali M. Sefidan, and Suvash C. Saha. Theoretical study on the performance of a solar still system integrated with pcm-pv module for sustainable water and power generation. *Desalination*, 443:184–197, 2018. ISSN 0011-9164. doi: https://doi.org/10.1016/j.desal.2018.05.024. URL https://www.sciencedirect.com/science/article/pii/S001191641732708X.

[7] Arash Nemati, Hossein Nami, and Mortaza Yari. Assessment of different configurations of solar energy driven organic flash cycles (ofcs) via exergy and exergoeconomic methodologies. *Renewable energy*, 115:1231–1248, 2018.

[8] Nathan S Lewis. Toward cost-effective solar energy use. *science*, 315(5813):798–801, 2007.

[9] Hui Song, Shunqin Luo, Hengming Huang, Bowen Deng, and Jinhua Ye. Solar-driven hydrogen production: Recent advances, challenges, and future perspectives. *ACS Energy Letters*, 7:1043–1065, 2022. URL `https://pubs.acs.org/doi/full/10.1021/acsenergylett.1c02591`.

[10] IEA. Global hydrogen review 2021, iea, paris, 2021. URL `https://www.iea.org/reports/global-hydrogen-review-2021`.

[11] Marco Martino, Concetta Ruocco, Eugenio Meloni, Pluton Pullumbi, and Vincenzo Palma. Main hydrogen production processes: An overview. *Catalysts*, 11(5):547, 2021.

[12] S.Z. Baykara. Experimental solar water thermolysis. *International Journal of Hydrogen Energy*, 29(14):1459–1469, 2004. ISSN 0360-3199. doi: https://doi.org/10.1016/j.ijhydene.2004.02.011. URL `https://www.sciencedirect.com/science/article/pii/S0360319904000898`.

[13] Ibrahim Dincer and Canan Acar. Review and evaluation of hydrogen production methods for better sustainability. *International journal of hydrogen energy*, 40(34): 11094–11111, 2015.

[14] Farid Safari and Ibrahim Dincer. A review and comparative evaluation of thermochemical water splitting cycles for hydrogen production. *Energy Conversion and Management*, 205:112182, 2020. ISSN 0196-8904. doi: https://doi.org/10.1016/j.enconman.2019.112182. URL `https://www.sciencedirect.com/science/article/pii/S0196890419311884`.

[15] Ibrahim Dincer. Green methods for hydrogen production. *International Journal of Hydrogen Energy*, 37(2):1954–1971, 2012. ISSN 0360-3199. doi: https://doi.org/10.1016/j.ijhydene.2011.03.173. URL `https://www.sciencedirect.com/science/article/pii/S0360319911019823`. 10th International Conference on Clean Energy 2010.

[16] Michele A Lewis and A Taylor. High temperature thermochemical processes. *DOE hydrogen program, annual progress report*, pages 182–185, 2006.

[17] Fatih Yilmaz and Reşat Selbaş. Thermodynamic performance assessment of solar based sulfur-iodine thermochemical cycle for hydrogen generation. *Energy*, 140:520–529, 2017. ISSN 0360-5442. doi: https://doi.org/10.1016/j.energy.2017.08.121. URL `https://www.sciencedirect.com/science/article/pii/S0360544217314962`.

[18] Mehdi Mehrpooya, Bahram Ghorbani, Arman Ekrataleshian, and Seyed Ali

Mousavi. Investigation of hydrogen production by sulfur-iodine thermochemical water splitting cycle using renewable energy source. *International Journal of Energy Research*, 45(10):14845–14869, 2021.

[19] Martin Khzouz and Evangelos I. Gkanas. Hydrogen technologies for mobility and stationary applications: Hydrogen production, storage and infrastructure development. In Mansour Al Qubeissi, Ahmad El-kharouf, and Hakan Serhad Soyhan, editors, *Renewable Energy*, chapter 13. IntechOpen, Rijeka, 2020. doi: 10.5772/intechopen.91676. URL `https://doi.org/10.5772/intechopen.91676`.

[20] Matthias Binder, Michael Kraussler, Matthias Kuba, and Markus Luisser. Hydrogen from biomass gasification, 2018. URL `https://www.iea.org/reports/global-hydrogen-review-2021`.

[21] Y Calzavara, C Joussot-Dubien, G Boissonnet, and S Sarrade. Evaluation of biomass gasification in supercritical water process for hydrogen production. *Energy conversion and management*, 46(4):615–631, 2005.

[22] Tigabwa Y Ahmed, Murni M Ahmad, Suzana Yusup, Abrar Inayat, and Zakir Khan. Mathematical and computational approaches for design of biomass gasification for hydrogen production: A review. *Renewable and Sustainable Energy Reviews*, 16(4): 2304–2315, 2012.

[23] Guanyi Chen, J Andries, Zhongyang Luo, and H Spliethoff. Biomass pyrolysis/gasification for product gas production: the overall investigation of parametric effects. *Energy conversion and management*, 44(11):1875–1884, 2003.

[24] Aitor Arregi, Maider Amutio, Gartzen Lopez, Javier Bilbao, and Martin Olazar. Evaluation of thermochemical routes for hydrogen production from biomass: A review. *Energy conversion and management*, 165:696–719, 2018.

[25] Prakash Parthasarathy and K Sheeba Narayanan. Hydrogen production from steam gasification of biomass: influence of process parameters on hydrogen yield–a review. *Renewable energy*, 66:570–579, 2014.

[26] Rami S El-Emam and Hasan Özcan. Comprehensive review on the techno-economics of sustainable large-scale clean hydrogen production. *Journal of Cleaner Production*, 220:593–609, 2019.

[27] Jan Baeyens, Huili Zhang, Jiapei Nie, Lise Appels, Raf Dewil, Renaud Ansart, and Yimin Deng. Reviewing the potential of bio-hydrogen production by fermentation. *Renewable and Sustainable Energy Reviews*, 131:110023, 2020.

[28] Bing Zhang, Sui-Xin Zhang, Rui Yao, Yong-Hong Wu, and Jie-Shan Qiu. Progress and prospects of hydrogen production: Opportunities and challenges. *Journal of Electronic Science and Technology*, 19(2):100080, 2021.

[29] HD Schilling, B Bonn, and U Krauss. Coal gasification: existing processes and new developments, london, graham &, 1981.

[30] Osamah Siddiqui and Ibrahim Dincer. A well to pump life cycle environmental impact assessment of some hydrogen production routes. *International Journal of Hydrogen Energy*, 44(12):5773–5786, 2019.

[31] Mengdi Ji and Jianlong Wang. Review and comparison of various hydrogen production methods based on costs and life cycle impact assessment indicators. *International Journal of Hydrogen Energy*, 46(78):38612–38635, 2021. ISSN 0360-3199. doi: https://doi.org/10.1016/j.ijhydene.2021.09.142. URL `https://www.sciencedirect.com/science/article/pii/S0360319921036697`.

[32] Kaihu Hou and Ronald Hughes. The kinetics of methane steam reforming over a ni/α-al2o catalyst. *Chemical Engineering Journal*, 82(1-3):311–328, 2001.

[33] B Parkinson, P Balcombe, JF Speirs, AD Hawkes, and K Hellgardt. Levelized cost of co 2 mitigation from hydrogen production routes. *Energy & environmental science*, 12(1):19–40, 2019.

[34] Chi-Hung Liao, Chao-Wei Huang, and Jeffrey Wu. Hydrogen production from semiconductor-based photocatalysis via water splitting. *Catalysts*, 2(4):490–516, 2012.

[35] Claude Lamy and Pierre Millet. A critical review on the definitions used to calculate the energy efficiency coefficients of water electrolysis cells working under near ambient temperature conditions. *Journal of Power Sources*, 447:227350, 2020. ISSN 0378-7753. doi: https://doi.org/10.1016/j.jpowsour.2019.227350. URL `https://www.sciencedirect.com/science/article/pii/S0378775319313436`.

[36] Furat Dawood, Martin Anda, and GM Shafiullah. Hydrogen production for energy: An overview. *International Journal of Hydrogen Energy*, 45(7):3847–3869, 2020.

[37] Mohd Fadhzir Ahmad Kamaroddin, Nordin Sabli, Pooria Moozarm Nia, Tuan Amran Tuan Abdullah, Luqman Chuah Abdullah, Shamsul Izhar, Adnan Ripin, and Arshad Ahmad. Phosphoric acid doped composite proton exchange membrane for hydrogen production in medium-temperature copper chloride electrolysis. *International Journal of Hydrogen Energy*, 45(42):22209–22222, 2020.

[38] Dia Milani, Ali Kiani, and Robbie McNaughton. Renewable-powered hydrogen economy from australia's perspective. *International Journal of Hydrogen Energy*, 45(46):24125–24145, 2020.

[39] Craig A Grimes, Oomman K Varghese, and Sudhir Ranjan. *Light, water, hydrogen: the solar generation of hydrogen by water photoelectrolysis*, volume 3. Springer, 2008.

[40] Iain Staffell, Daniel Scamman, Anthony Velazquez Abad, Paul Balcombe, Paul E Dodds, Paul Ekins, Nilay Shah, and Kate R Ward. The role of hydrogen and fuel cells in the global energy system. *Energy & Environmental Science*, 12(2):463–491, 2019.

[41] Roxanne Pinsky, Piyush Sabharwall, Jeremy Hartvigsen, and James O'Brien. Comparative review of hydrogen production technologies for nuclear hybrid energy systems. *Progress in Nuclear Energy*, 123:103317, 2020.

[42] Changqing Li and Jong-Beom Baek. The promise of hydrogen production from alkaline anion exchange membrane electrolyzers. *Nano Energy*, 87:106162, 2021.

[43] Alfredo Ursua, Luis M Gandia, and Pablo Sanchis. Hydrogen production from water electrolysis: current status and future trends. *Proceedings of the IEEE*, 100 (2):410–426, 2011.

[44] Immanuel Vincent and Dmitri Bessarabov. Low cost hydrogen production by anion exchange membrane electrolysis: A review. *Renewable and Sustainable Energy Reviews*, 81:1690–1704, 2018.

[45] Long Chen, Xiaoli Dong, Yonggang Wang, and Yongyao Xia. Separating hydrogen and oxygen evolution in alkaline water electrolysis using nickel hydroxide. *Nature communications*, 7(1):1–8, 2016.

[46] Jamie D Holladay, Jianli Hu, David L King, and Yong Wang. An overview of hydrogen production technologies. *Catalysis today*, 139(4):244–260, 2009.

[47] Seyed Ehsan Hosseini and Mazlan Abdul Wahid. Hydrogen from solar energy, a clean energy carrier from a sustainable source of energy. *International Journal of Energy Research*, 44(6):4110–4131, 2020.

[48] MA Laguna-Bercero. Recent advances in high temperature electrolysis using solid oxide fuel cells: A review. *Journal of Power sources*, 203:4–16, 2012.

[49] Zhengping Zhou, Oksana Zholobko, Xiang-Fa Wu, Ted Aulich, Jivan Thakare, and

John Hurley. Polybenzimidazole-based polymer electrolyte membranes for high-temperature fuel cells: current status and prospects. *Energies*, 14(1):135, 2021.

[50] Omar J Guerra, Josh Eichman, Bri-Mathias Hodge, and Jennifer Kurtz. *Cost-Competitive Electrolysis-Based Hydrogen Under Current US Electric Utility Rates*. National Renewable Energy Laboratory, 2018.

[51] Yoongu Lim, Dong-Kyu Lee, Seong Min Kim, Woosung Park, Sung Yong Cho, and Uk Sim. Low dimensional carbon-based catalysts for efficient photocatalytic and photo/electrochemical water splitting reactions. *Materials*, 13(1):114, 2020.

[52] Osama Al-Madanat, Yamen AlSalka, Wegdan Ramadan, and Detlef W Bahnemann. Tio2 photocatalysis for the transformation of aromatic water pollutants into fuels. *Catalysts*, 11(3):317, 2021.

[53] Elnaz Bahadori, Gianguido Ramis, Danny Zanardo, Federica Menegazzo, Michela Signoretto, Delia Gazzoli, Daniela Pietrogiacomi, Alessandro Di Michele, and Ilenia Rossetti. Photoreforming of glucose over cuo/tio2. *Catalysts*, 10(5):477, 2020.

[54] Xie Quan, Shaogui Yang, Xiuli Ruan, and Huiming Zhao. Preparation of titania nanotubes and their environmental applications as electrode. *Environmental science & technology*, 39(10):3770–3775, 2005.

[55] Jennyffer Martinez Quimbayo, Satu Ojala, Samuli Urpelainen, Mika Huuhtanen, Wei Cao, Marko Huttula, and Riitta L Keiski. Nanostructured photocatalytic materials for water purification. In *Advanced Oxidation Processes for Wastewater Treatment*, pages 249–270. CRC Press, 2022.

[56] Yohei Tanaka, Kiyoshi Matsuo, and Shunsuke Yuzuriha. Long-lasting muscle thinning induced by infrared irradiation specialized with wavelengths and contact cooling: a preliminary report. *Eplasty*, 10, 2010.

[57] Huan Zhang, Qin-Qin Gu, Yi-Wen Zhou, Shou-Qing Liu, Wen-Xiao Liu, Li Luo, and Ze-Da Meng. Direct z-scheme photocatalytic removal of ammonia via the narrow band gap mos2/n-doped graphene hybrid catalyst upon near-infrared irradiation. *Applied Surface Science*, 504:144065, 2020. ISSN 0169-4332. doi: https://doi.org/10.1016/j.apsusc.2019.144065. URL `https://www.sciencedirect.com/science/article/pii/S0169433219328818`.

[58] Kelly S. Potter and Joseph H. Simmons. Chapter 6 - energy-related optical materials. In Kelly S. Potter and Joseph H. Simmons, editors, *Optical Materials (Second Edition)*, pages 309–368. Elsevier, second edition edition, 2021. ISBN 978-0-12-

818642-8. doi: https://doi.org/10.1016/B978-0-12-818642-8.00006-5. URL `https://www.sciencedirect.com/science/article/pii/B9780128186428000065`.

[59] Josep Albero, Diego Mateo, and Hermenegildo García. Graphene-based materials as efficient photocatalysts for water splitting. *Molecules*, 24(5):906, 2019.

[60] Stefano Lettieri, Michele Pavone, Ambra Fioravanti, Luigi Santamaria Amato, and Pasqualino Maddalena. Charge carrier processes and optical properties in tio2 and tio2-based heterojunction photocatalysts: A review. *Materials*, 14(7):1645, 2021.

[61] Pablo Ayala, Ariane Giesriegl, Sreejith P Nandan, Stephen Nagaraju Myakala, Peter Wobrauschek, and Alexey Cherevan. Isolation strategy towards earth-abundant single-site co-catalysts for photocatalytic hydrogen evolution reaction. *Catalysts*, 11 (4):417, 2021.

[62] Zhongliao Wang, Jiajie Fan, Bei Cheng, Jiaguo Yu, and Jingsan Xu. Nickel-based cocatalysts for photocatalysis: Hydrogen evolution, overall water splitting and co2 reduction. *Materials Today Physics*, 15:100279, 2020.

[63] Boglárka Hampel, Zsolt Pap, Andras Sapi, Akos Szamosvolgyi, Lucian Baia, and Klara Hernadi. Application of tio2-cu composites in photocatalytic degradation different pollutants and hydrogen production. *Catalysts*, 10(1):85, 2020.

[64] Parisa Talebi, Harishchandra Singh, Ekta Rani, Marko Huttula, and Wei Cao. Surface plasmon-driven photocatalytic activity of ni@ nio/nico 3 core–shell nanostructures. *RSC Advances*, 11(5):2733–2743, 2021.

[65] Shireen Meher Kotay and Debabrata Das. Biohydrogen as a renewable energy resource—prospects and potentials. *International Journal of Hydrogen Energy*, 33 (1):258–263, 2008.

[66] CNC Hitam and AA Jalil. A review on biohydrogen production through photofermentation of lignocellulosic biomass. *Biomass Conversion and Biorefinery*, pages 1–19, 2020.

[67] Femina Carolin Christopher, P Senthil Kumar, Dai-Viet N Vo, and G Janet Joshiba. A review on critical assessment of advanced bioreactor options for sustainable hydrogen production. *International Journal of Hydrogen Energy*, 46(10):7113–7136, 2021.

[68] Kaushik Nath and Debabrata Das. Improvement of fermentative hydrogen production: various approaches. *Applied microbiology and biotechnology*, 65(5):520–529, 2004.

[69] Jin Hyun Kim, Dharmesh Hansora, Pankaj Sharma, Ji-Wook Jang, and Jae Sung Lee. Toward practical solar hydrogen production–an artificial photosynthetic leaf-to-farm challenge. *Chemical Society Reviews*, 48(7):1908–1971, 2019.

[70] G Olalde, D Gauthier, A Vialaron, and L Fulcheri. New solar system for water thermolysis with a high energetic yield. In *Intersol Eighty Five*, pages 1927–1931. Elsevier, 1986.

[71] E Bilgen, J Galindo, and SZ Baykara. Experimental study of hydrogen production by direct decomposition of water. In *IECEC'83; Proceedings of the Eighteenth Intersociety Energy Conversion Engineering Conference, Volume 1*, volume 2, pages 564–568, 1983.

[72] Mehdi Mehrpooya, Bahram Ghorbani, and Mohammadmahdi Khodaverdi. Hydrogen production by thermochemical water splitting cycle using low-grade solar heat and phase change material energy storage system. *International Journal of Energy Research*, 2022.

[73] Shayan Sadeghi and Samane Ghandehariun. A standalone solar thermochemical water splitting hydrogen plant with high-temperature molten salt: Thermodynamic and economic analyses and multi-objective optimization. *Energy*, 240:122723, 2022. ISSN 0360-5442. doi: https://doi.org/10.1016/j.energy.2021.122723. URL `https://www.sciencedirect.com/science/article/pii/S0360544221029728`.

[74] Rahul R. Bhosale. Solar hydrogen production via zno/zn based thermochemical water splitting cycle: Effect of partial reduction of zno. *International Journal of Hydrogen Energy*, 46(6):4739–4748, 2021. ISSN 0360-3199. doi: https://doi.org/10.1016/j.ijhydene.2020.02.135. URL `https://www.sciencedirect.com/science/article/pii/S0360319920307163`. Special issue on Selected Contributions from the 8th Global Conference on Global Warming (GCGW-2019), 22-25 April 2019, Doha, Qatar.

[75] Rahul Bhosale, Anand Kumar, Fares AlMomani, and Ram B. Gupta. Solar thermochemical zno/znso4 water splitting cycle for hydrogen production. *International Journal of Hydrogen Energy*, 42(37):23474–23483, 2017. ISSN 0360-3199. doi: https://doi.org/10.1016/j.ijhydene.2017.02.190. URL `https://www.sciencedirect.com/science/article/pii/S0360319917307723`. Special Issue on The 1st International Conference on Advanced Energy Materials (AEM2016), 12-14 September 2016, Surrey, England.

[76] Rahul R. Bhosale, Anand Kumar, and Parag Sutar. Thermodynamic analy-

sis of solar driven sno2/sno based thermochemical water splitting cycle. *Energy Conversion and Management*, 135:226–235, 2017. ISSN 0196-8904. doi: https://doi.org/10.1016/j.enconman.2016.12.067. URL https://www.sciencedirect.com/science/article/pii/S0196890416311591.

[77] Francesco Patuzzi, Daniele Basso, Stergios Vakalis, Daniele Antolini, Stefano Piazzi, Vittoria Benedetti, Eleonora Cordioli, and Marco Baratieri. State-of-the-art of small-scale biomass gasification systems: An extensive and unique monitoring review. *Energy*, 223:120039, 2021. ISSN 0360-5442. doi: https://doi.org/10.1016/j.energy.2021.120039. URL https://www.sciencedirect.com/science/article/pii/S0360544221002887.

[78] Penghua Qiu, Changshuai Du, Li Liu, and Lei Chen. Hydrogen and syngas production from catalytic steam gasification of char derived from ion-exchangeable na- and ca-loaded coal. *International Journal of Hydrogen Energy*, 43(27):12034–12048, 2018. ISSN 0360-3199. doi: https://doi.org/10.1016/j.ijhydene.2018.04.055. URL https://www.sciencedirect.com/science/article/pii/S0360319918311807.

[79] Yongliang Yan, Dhinesh Thanganadar, Peter T. Clough, Sanjay Mukherjee, Kumar Patchigolla, Vasilije Manovic, and Edward J. Anthony. Process simulations of blue hydrogen production by upgraded sorption enhanced steam methane reforming (se-smr) processes. *Energy Conversion and Management*, 222:113144, 2020. ISSN 0196-8904. doi: https://doi.org/10.1016/j.enconman.2020.113144. URL https://www.sciencedirect.com/science/article/pii/S0196890420306889.

[80] Jörn Brauns and Thomas Turek. Alkaline water electrolysis powered by renewable energy: A review. *Processes*, 8(2):248, 2020.

[81] Kewei Hu, Jiakun Fang, Xiaomeng Ai, Danji Huang, Zhiyao Zhong, Xiaobo Yang, and Lei Wang. Comparative study of alkaline water electrolysis, proton exchange membrane water electrolysis and solid oxide electrolysis through multiphysics modeling. *Applied Energy*, 312:118788, 2022. ISSN 0306-2619. doi: https://doi.org/10.1016/j.apenergy.2022.118788. URL https://www.sciencedirect.com/science/article/pii/S0306261922002367.

[82] S. Campagna Zignani, M. Lo Faro, A. Carbone, C. Italiano, S. Trocino, G. Monforte, and A.S. Aricò. Performance and stability of a critical raw materials-free anion exchange membrane electrolysis cell. *Electrochimica Acta*, 413:140078, 2022. ISSN 0013-4686. doi: https://doi.org/10.1016/j.electacta.2022.140078. URL https://www.sciencedirect.com/science/article/pii/S001346862200250X.

[83] Jaromír Hnát, Martin Paidar, and Karel Bouzek. 5 - hydrogen production by electrolysis. In Adolfo Iulianelli and Angelo Basile, editors, *Current Trends and Future Developments on (Bio-) Membranes*, pages 91–117. Elsevier, 2020. ISBN 978-0-12-817384-8. doi: https://doi.org/10.1016/B978-0-12-817384-8.00005-4. URL `https://www.sciencedirect.com/science/article/pii/B9780128173848000054`.

[84] Pengzuo Chen and Xile Hu. High-efficiency anion exchange membrane water electrolysis employing non-noble metal catalysts. *Advanced Energy Materials*, 10(39): 2002285, 2020.

[85] Yoo Sei Park, Jooyoung Lee, Myeong Je Jang, Juchan Yang, Jaehoon Jeong, Jaeho Park, Yangdo Kim, Min Ho Seo, Zhongwei Chen, and Sung Mook Choi. High-performance anion exchange membrane alkaline seawater electrolysis. *Journal of Materials Chemistry A*, 9(15):9586–9592, 2021.

[86] S. Jayachitra, D. Mahendiran, P. Ravi, P. Murugan, and M. Sathish. Highly conductive nise2 nanoparticle as a co-catalyst over tio2 for enhanced photocatalytic hydrogen production. *Applied Catalysis B: Environmental*, 307:121159, 2022. ISSN 0926-3373. doi: https://doi.org/10.1016/j.apcatb.2022.121159. URL `https://www.sciencedirect.com/science/article/pii/S0926337322000996`.

[87] Yongjie Wang, Yuanpeng Wu, Kai Sun, and Zetian Mi. A quadruple-band metal–nitride nanowire artificial photosynthesis system for high efficiency photocatalytic overall solar water splitting. *Materials Horizons*, 6(7):1454–1462, 2019.

[88] MG Kibria, FA Chowdhury, S Zhao, B AlOtaibi, ML Trudeau, H Guo, and Z Mi. Visible light-driven efficient overall water splitting using p-type metal-nitride nanowire arrays. *Nature communications*, 6(1):1–8, 2015.

[89] Haowen Feng, Chihe Sun, Chaofan Zhang, Haixing Chang, Nianbing Zhong, Wenbo Wu, Haihua Wu, Xuefei Tan, Mengying Zhang, and Shih-Hsin Ho. Bioconversion of mature landfill leachate into biohydrogen and volatile fatty acids via microalgal photosynthesis together with dark fermentation. *Energy Conversion and Management*, 252:115035, 2022. ISSN 0196-8904. doi: https://doi.org/10.1016/j.enconman.2021.115035. URL `https://www.sciencedirect.com/science/article/pii/S0196890421012115`.

[90] Hong Chen, Jun Wu, Rong Huang, Wenzhe Zhang, Weining He, Zhengyu Deng, Yunping Han, Benyi Xiao, Hongmei Luo, and Wei Qu. Effects of temperature and total solid content on biohydrogen production from dark fermentation of rice straw: Performance and microbial community characteristics. *Chemosphere*,

286:131655, 2022. ISSN 0045-6535. doi: https://doi.org/10.1016/j.chemosphere.2021.131655. URL https://www.sciencedirect.com/science/article/pii/S0045653521021275.

[91] Chaoyang Lu, Danping Jiang, Yanyan Jing, Zhiping Zhang, Xiaoyu Liang, Jianzhi Yue, Yameng Li, Huan Zhang, Yang Zhang, Kaixin Wang, Ningyuan Zhang, and Quanguo Zhang. Enhancing photo-fermentation biohydrogen production from corn stalk by iron ion. *Bioresource Technology*, 345:126457, 2022. ISSN 0960-8524. doi: https://doi.org/10.1016/j.biortech.2021.126457. URL https://www.sciencedirect.com/science/article/pii/S0960852421017995.

[92] Sharma Mona, Smita S. Kumar, Vivek Kumar, Khalida Parveen, Neha Saini, Bansal Deepak, and Arivalagan Pugazhendhi. Green technology for sustainable biohydrogen production (waste to energy): A review. *Science of The Total Environment*, 728:138481, 2020. ISSN 0048-9697. doi: https://doi.org/10.1016/j.scitotenv.2020.138481. URL https://www.sciencedirect.com/science/article/pii/S004896972031994X.

[93] Jieyang Jia, Linsey C Seitz, Jesse D Benck, Yijie Huo, Yusi Chen, Jia Wei Desmond Ng, Taner Bilir, James S Harris, and Thomas F Jaramillo. Solar water splitting by photovoltaic-electrolysis with a solar-to-hydrogen efficiency over 30%. *Nature communications*, 7(1):1–6, 2016.

[94] Shu Hu, Chengxiang Xiang, Sophia Haussener, Alan D Berger, and Nathan S Lewis. An analysis of the optimal band gaps of light absorbers in integrated tandem photoelectrochemical water-splitting systems. *Energy & Environmental Science*, 6(10): 2984–2993, 2013.

[95] Akira Fujishima and Kenichi Honda. Electrochemical photolysis of water at a semiconductor electrode. *nature*, 238(5358):37–38, 1972.

[96] J. Fernández-Catalá, G. Garrigós-Pastor, Á. Berenguer-Murcia, and D. Cazorla-Amorós. Photo-microfluidic chip reactors for propene complete oxidation with tio2 photocalyst using uv-led light. *Journal of Environmental Chemical Engineering*, 7(5):103408, 2019. ISSN 2213-3437. doi: https://doi.org/10.1016/j.jece.2019.103408. URL https://www.sciencedirect.com/science/article/pii/S2213343719305317.

[97] Mohammad Mansoob Khan, Syed Farooq Adil, and Abdullah Al-Mayouf. Metal oxides as photocatalysts, 2015.

[98] Javier Fernández-Catalá, Ángel Berenguer-Murcia, and Diego Cazorla-Amorós.

Photocatalytic oxidation of vocs in gas phase using capillary microreactors with commercial tio2 (p25) fillings. *Materials*, 11(7), 2018. ISSN 1996-1944. doi: 10.3390/ma11071149. URL https://www.mdpi.com/1996-1944/11/7/1149.

[99] Jining Zhang, Yifan Lei, Shuang Cao, Wenping Hu, Lingyu Piao, and Xiaobo Chen. Photocatalytic hydrogen production from seawater under full solar spectrum without sacrificial reagents using tio2 nanoparticles. *Nano Research*, 15(3):2013–2022, 2022.

[100] Sundaram Chandrasekaran, Lei Yao, Libo Deng, Chris Bowen, Yan Zhang, Sanming Chen, Zhiqun Lin, Feng Peng, and Peixin Zhang. Recent advances in metal sulfides: from controlled fabrication to electrocatalytic, photocatalytic and photoelectrochemical water splitting and beyond. *Chemical Society Reviews*, 48(15): 4178–4280, 2019.

[101] Zizhan Liang, Rongchen Shen, Yun Hau Ng, Peng Zhang, Quanjun Xiang, and Xin Li. A review on 2d mos2 cocatalysts in photocatalytic h2 production. *Journal of Materials Science & Technology*, 56:89–121, 2020. ISSN 1005-0302. doi: https://doi.org/10.1016/j.jmst.2020.04.032. URL https://www.sciencedirect.com/science/article/pii/S1005030220303844. Solar-driven Photocatalystic Materials.

[102] Sergio San Martín, Maria J Rivero, and Inmaculada Ortiz. Unravelling the mechanisms that drive the performance of photocatalytic hydrogen production. *Catalysts*, 10(8):901, 2020.

[103] David Ramírez-Ortega, Próspero Acevedo-Peña, Francisco Tzompantzi, Rubén Arroyo, Federico González, and Ignacio González. Energetic states in sno2–tio2 structures and their impact on interfacial charge transfer process. *Journal of Materials Science*, 52(1):260–275, 2017.

[104] Guangzhao Wang, Wenyi Tang, Wenjie Xie, Qin Tang, Yongtong Wang, Hao Guo, Peng Gao, Suihu Dang, and Junli Chang. Type-ii cds/ptsse heterostructures used as highly efficient water-splitting photocatalysts. *Applied Surface Science*, page 152931, 2022.

[105] Jiajia Liu, Yanqing Shen, Lingling Lv, Xianghui Meng, Xu Gao, Min Zhou, Yangdong Zheng, and Zhongxiang Zhou. Rational design direct z-scheme β-gese/hfs2 heterostructure by interfacial engineering: efficient photocatalyst for overall water splitting in the wide solar spectrum. *Applied Surface Science*, page 153025, 2022.

[106] Peng Lu, Xueli Hu, Yujie Li, Yazhou Peng, Meng Zhang, Xue Jiang, Youzhou

He, Min Fu, Fan Dong, and Zhi Zhang. Novel caco3/g-c3n4 composites with enhanced charge separation and photocatalytic activity. *Journal of Saudi Chemical Society*, 23(8):1109–1118, 2019. ISSN 1319-6103. doi: https://doi.org/10.1016/j.jscs.2019.07.002. URL https://www.sciencedirect.com/science/article/pii/S1319610319300754.

[107] Jiuqing Wen, Jun Xie, Xiaobo Chen, and Xin Li. A review on g-c3n4-based photocatalysts. *Applied Surface Science*, 391:72–123, 2017. ISSN 0169-4332. doi: https://doi.org/10.1016/j.apsusc.2016.07.030. URL https://www.sciencedirect.com/science/article/pii/S016943321631457X. 2nd International Symposium on Energy and Environmental Photocatalytic Materials.

[108] Jinyuan Liu, Yanhua Song, Hui Xu, Xingwang Zhu, Jiabiao Lian, Yuanguo Xu, Yan Zhao, Liying Huang, Haiyan Ji, and Huaming Li. Non-metal photocatalyst nitrogen-doped carbon nanotubes modified mpg-c3n4: facile synthesis and the enhanced visible-light photocatalytic activity. *Journal of Colloid and Interface Science*, 494: 38–46, 2017. ISSN 0021-9797. doi: https://doi.org/10.1016/j.jcis.2017.01.010. URL https://www.sciencedirect.com/science/article/pii/S0021979717300103.

[109] Chunmei Bai, Jin Xiang, Zilong Zhao, Shuwen Luo, and Liang Li. Improvement of hydrogen production performance by in situ doping of carbon nanotubes into tio2 materials. *Journal of Nanoparticle Research*, 24(3):1–9, 2022.

[110] Zhi-An Lan, Xu Chi, Meng Wu, Xirui Zhang, Xiong Chen, Guigang Zhang, and Xinchen Wang. Molecular design of covalent triazine frameworks with anisotropic charge migration for photocatalytic hydrogen production. *Small*, page 2200129, 2022.

[111] Dan Kong, Yun Zheng, Marcin Kobielusz, Yiou Wang, Zhiming Bai, Wojciech Macyk, Xinchen Wang, and Junwang Tang. Recent advances in visible light-driven water oxidation and reduction in suspension systems. *Materials Today*, 21(8):897–924, 2018. ISSN 1369-7021. doi: https://doi.org/10.1016/j.mattod.2018.04.009. URL https://www.sciencedirect.com/science/article/pii/S1369702117308635.

[112] Jieying Jing, Jing Li, Jie Feng, Wenying Li, and William W. Yu. Photodegradation of quinoline in water over magnetically separable fe3o4/tio2 composite photocatalysts. *Chemical Engineering Journal*, 219:355–360, 2013. ISSN 1385-8947. doi: https://doi.org/10.1016/j.cej.2012.12.058. URL https://www.sciencedirect.com/science/article/pii/S1385894712017081.

[113] Bo Chen, Sijiang Chen, Harshad A. Bandal, Richard Appiah-Ntiamoah, Amol R.

Jadhav, and Hern Kim. Cobalt nanoparticles supported on magnetic core-shell structured carbon as a highly efficient catalyst for hydrogen generation from nabh4 hydrolysis. *International Journal of Hydrogen Energy*, 43(19):9296–9306, 2018. ISSN 0360-3199. doi: https://doi.org/10.1016/j.ijhydene.2018.03.193. URL `https://www.sciencedirect.com/science/article/pii/S0360319918310267`.

[114] Jorge Bedia, Virginia Muelas-Ramos, Manuel Peñas-Garzón, Almudena Gómez-Avilés, Juan J Rodríguez, and Carolina Belver. A review on the synthesis and characterization of metal organic frameworks for photocatalytic water purification. *Catalysts*, 9(1):52, 2019.

[115] Shengjun Liu, Cheng Zhang, Yudie Sun, Qian Chen, Lifang He, Kui Zhang, Jian Zhang, Bo Liu, and Li-Feng Chen. Design of metal-organic framework-based photocatalysts for hydrogen generation. *Coordination Chemistry Reviews*, 413:213266, 2020. ISSN 0010-8545. doi: https://doi.org/10.1016/j.ccr.2020.213266. URL `https://www.sciencedirect.com/science/article/pii/S0010854520300163`.

[116] Jian-Jian Zhou, Rong Wang, Xin-Ling Liu, Fu-Min Peng, Chuan-Hao Li, Fei Teng, and Yu-Peng Yuan. In situ growth of cds nanoparticles on uio-66 metal-organic framework octahedrons for enhanced photocatalytic hydrogen production under visible light irradiation. *Applied Surface Science*, 346:278–283, 2015.

[117] Haiyan Nan, Zilu Wang, Wenhui Wang, Zheng Liang, Yan Lu, Qian Chen, Daowei He, Pingheng Tan, Feng Miao, Xinran Wang, et al. Strong photoluminescence enhancement of mos2 through defect engineering and oxygen bonding. *ACS nano*, 8(6):5738–5745, 2014.

[118] Haixi Pan, Liping Feng, Pengfei Liu, Xiaoqi Zheng, and Xiaodong Zhang. Asymmetric surfaces endow janus bismuth oxyhalides with enhanced electronic and catalytic properties for the hydrogen evolution reaction. *Journal of Colloid and Interface Science*, 2022.

[119] Stefan Pfenninger and Iain Staffell. Long-term patterns of european pv output using 30 years of validated hourly reanalysis and satellite data. *Energy*, 114:1251–1265, 2016.

[120] Stefan Pfenninger and Iain Staffell. Renewables. ninja. *URL https://www. renewables. ninja*, 2016.

[121] Elena Crespi, Paolo Colbertaldo, Giulio Guandalini, and Stefano Campanari. Design of hybrid power-to-power systems for continuous clean pv-based energy supply. *International Journal of Hydrogen Energy*, 46(26):13691–13708, 2021.

[122] Daniel Lugo-Laguna, Angel Arcos-Vargas, and Fernando Nuñez-Hernandez. A european assessment of the solar energy cost: Key factors and optimal technology. *Sustainability*, 13(6):3238, 2021.

[123] Fernando Núñez, David Canca, and Ángel Arcos-Vargas. An assessment of european electricity arbitrage using storage systems. *Energy*, 242:122916, 2022.

[124] Statistics Finland. Inflation rate in finland. *URL https://www.stat.fi*, 2021.

[125] Statistics Finland. Energy prices in finland. *URL https://www.stat.fi*, 2021.

[126] Pietari Puranen, Antti Kosonen, and Jero Ahola. Techno-economic viability of energy storage concepts combined with a residential solar photovoltaic system: A case study from finland. *Applied Energy*, 298:117199, 2021.

[127] Dentons. Italy: New incentives regime for renewable energy plants. *URL https://www.dentons.com*, 2020.

[128] Tsuyoshi Takata, Junzhe Jiang, Yoshihisa Sakata, Mamiko Nakabayashi, Naoya Shibata, Vikas Nandal, Kazuhiko Seki, Takashi Hisatomi, and Kazunari Domen. Photocatalytic water splitting with a quantum efficiency of almost unity. *Nature*, 581(7809):411–414, 2020.

[129] K.G.U. Wijayatha. 5 - photoelectrochemical cells for hydrogen generation. In John A. Kilner, Stephen J. Skinner, Stuart J.C. Irvine, and Peter P. Edwards, editors, *Functional Materials for Sustainable Energy Applications*, Woodhead Publishing Series in Energy, pages 91–146e. Woodhead Publishing, 2012. ISBN 978-0-85709-059-1. doi: https://doi.org/10.1533/9780857096371.1.91. URL `https://www.sciencedirect.com/science/article/pii/B9780857090591500051`.

List of Figures

List of Tables

List of Symbols

Variable	Description	SI unit
$\boldsymbol{H}$	Enthalpy of formation	kJ/mol
$\boldsymbol{T}$	Temperature	K
$\boldsymbol{LHV}$	Lower heating value	kWh/kg
$\boldsymbol{h}$	Plank constant	m^2kg/s
$\boldsymbol{\nu}$	Frequency	1/s
$\boldsymbol{\eta}$	Efficiency	%
$\boldsymbol{STH}$	Solar-to-hydrogen conversion efficiency	%
$\boldsymbol{E}$	Energy	kWh
$\boldsymbol{w}$	Specific work	kJ/kg
$\boldsymbol{P}$	Power	kW
$\boldsymbol{i}$	Component	-
$\boldsymbol{I}$	Cost	€
$\boldsymbol{CAPEX}$	Investment cost	€
$\boldsymbol{OPEX}$	Operating cost	€
$\boldsymbol{T_t}$	Tax rate	%
$\boldsymbol{r}$	Inflation rate	%
$\boldsymbol{C}$	Unit cost	€/unit
$\boldsymbol{r}_{H_2}$	Hydrogen evolution rate	mol/s
$\boldsymbol{G}$	Gibbs free energy	kJ/mol
$\boldsymbol{A}$	Area	m^2
$\boldsymbol{I_{solar}}$	Light energy flux	kW/m^2

Acknowledgements

For sure, this project would not have been possible without the support of my supervisors. Thank you Prof. Giulio Guandalini and Adj. Prof. Samuli Urpelainen for your patience, guidance, support, and brilliant comments on numerous revisions of this thesis. I sincerely acknowledge the assistance from all people from NANOMO research unit at the University of Oulu. In particular, I would like to say thank you to Dr. Rossella Greco for her help with the Italian abstract.